1

The initial mass function of stars and the star-formation rates of galaxies

Pavel Kroupa^a and Tereza Jerabkova^b

(This is Chapter 2 in the book "Star-formation Rates of Galaxies", edited by Veronique Buat & Andreas Zezas, published in April 2021 by Cambridge University Press [ISBN: 9781107184169]. This arXiv version contains additional material in Sec. 1.1.1, 1.1.2, 1.2, 1.3 and 1.7.1.)

Abstract

The measured star-formation rates (SFRs) of galaxies comprise an important constraint on galaxy evolution and also on their cosmological boundary conditions. Any available tracer of the SFR depends on the shape of the mass-distribution of formed stars, i.e. on the stellar initial mass function (IMF). The luminous massive stars dominate the observed photon flux while the dim low-mass stars dominate the mass in the freshly formed population. Errors in the number ratio of the massive to low-mass stars lead to errors in SFR measurements and thus to errors concerning the gas-accretion-rates and the gas-consumption time-scales of galaxies. The stellar IMF has traditionally been interpreted to be a scale-invariant probability density distribution function (PDF), but it may instead be an optimal distribution function. In the PDF interpretation, the stellar IMF observed on the stales of individual star clusters is equal to the galaxy-wide IMF (gwIMF) which, by implication, would be invariant. In this Chapter we discuss the fundamental properties of the IMF and of the gwIMF, the nature of both and their systematic variability as indicated by measurements and theoretical expectations, and we discuss the implications for the SFRs of galaxies and on their main sequence. The importance of the putative most-massive-starmass vs stellar-mass-of-the- hosting-embedded-cluster $(m_{\text{max}} - M_{\text{ecl}})$ relation and its possible establish- ment during the proto-stellar formation phase, is emphasised.

^a Helmholtz-Institut für Strahlen- und Kernphysik, Nussallee 14-16, 53115 Bonn, Germany; Charles University in Prague, Faculty of Mathematics and Physics, Astronomical Institute, V Holešovičkách 2, CZ-18000 Praha, Czech Republic; pavel.kroupa@mff.cuni.cz

 $[^]b$ ESA Fellow; ESTEC/SCI-S, Keplerlaan 1, 2200 AG Noordwijk, Netherlands; tereza.jerabkova@esa.int

1.1 Introduction

Let dN be the number of stars in the infinitesimal initial-stellar-mass interval m to m+dm, then $dN=\xi(m)\,dm$ where $\xi(m)$ is the stellar IMF, that is, the distribution of the initial masses of all stars formed together. It is usual to represent the IMF with a power-law function, $\xi(m) \propto m^{-\alpha_i}$, where the power-law indices depend on the mass range considered and $\alpha_S=2.35$ is the Salpeter index valid for the mass range $0.4\,M_{\odot}-10\,M_{\odot}$ (Salpeter, 1955).

It follows that it is in principle straight-forward to construct $\xi(m)$ because the astronomer merely needs to look up and count the stars. The difficulty in the practical execution of this is that stellar masses are only measurable directly when they are in binary orbits. For the vast majority of stars binary-orbits are not available though, and their masses can only be inferred from their luminosities, colours and spectra relying on theoretical stellar models. Theoretical models assign these radiant properties a mass, provided an age, stellar spin and chemical abundance is known, these properties of the star being also measured from similar data. Massive stars are extremely luminous and shine mostly in the UV with a steep mass-luminosity relation, while low-mass stars are dim and shine largely in the red and infrared with a flat mass-luminosity relation (small uncertainties in the mass translate into large uncertainties in the luminosity). Massive stars are rare and live only for a few Myr while low mass stars dominate the population in numbers and live up to many Hubble times.

The practical construction from observational data of the IMF over all stellar masses is thus subject to very major uncertainties requiring data from different surveys to be put together. This is particularly true for the Galactic field stellar ensemble nearby to the Sun, where a complete census of the massive stars is reachable to distances of a few kpc but the low-mass stars can only be detected to within a few pc (Sec. 1.3).

To infer the stellar IMF in the Galactic field the massive-star and low-mass star counts need to be combined appropriately and carefully which requires taking care of the different spatial distribution and the star formation history (Salpeter, 1955; Miller and Scalo, 1979; Scalo, 1986; Elmegreen and Scalo, 2006). The surveys of stars in star clusters do not suffer from this complication since the stars are practically at the same distance, clusters typically being further than a few dozen pc away from us while their radii are typically 3 pc, and the stars have nearly the same ages. One problem with star clusters though is that stellar-dynamical processes remove stars from the clusters already starting at the earliest times (a few 10⁵ yr) (Baumgardt and Makino, 2003; Banerjee and Kroupa, 2012; Haghi et al., 2015; Oh et al.,

2015; Oh and Kroupa, 2016; Kroupa et al., 2018), binary-star evolution and dynamically-induced stellar mergers also affect the inferred IMF (de Mink et al., 2014; Schneider et al., 2015; Oh and Kroupa, 2018). Also, and in all cases, in the Galactic field, star clusters and any other stellar ensemble, the star counts always suffer from unresolved multiple systems such that the observer misses the fainter or unresolved companion. This bias is very significant for late-type stars (Kroupa et al., 1991) but is less problematical for more massive stars (Weidner et al., 2009; Kroupa and Jerabkova, 2018).

Given its important role in much of astrophysics, the IMF has been the subject of a vast research effort. Some relevant IMF-related questions that have been being addressed are: Can the IMF be measured? What is the shape of the IMF? What is its mathematical nature (e.g., is it a probability density distribution function)? Does the IMF vary? Does the IMF of a simple stellar population equal that of a composite population?

Reviews which address these questions can be found in Kroupa (2002b); Chabrier (2003); Bastian et al. (2010); Offner et al. (2014); Kroupa and Jerabkova (2018). The major effort to assess the IMF for stars more massive than a few M_{\odot} by Massey (2003) needs to be emphasised. The reviews by Kroupa et al. (2013) and particularly Hopkins (2018) cover the significant extra-galactic evidence for a variable galaxy-wide IMF. Here we address these five most-important IMF questions in turn and place them into the context of the determination of the SFRs of galaxies. Needless to write, the answers to these questions have a rather major impact on the SFRs which are calculated given some tracer. This in turn affects our knowledge and understanding of the matter cycle in the Universe.

The IMF is the key to understanding the cosmological matter cycle.

In the following two sub-sections we explain some IMF-acronyms and discuss some issues concerning how stars emerge from the inter-stellar medium.

1.1.1 Used IMF terminology throughout this text

Throughout this text we define several acronyms describing the IMF on different scales. It is useful to introduce these once a variable non-universal IMF is discussed (Hopkins, 2018; Jeřábková et al., 2018).

As in Jeřábková et al. (2018) we refer to the *IMF* as being the stellar initial mass function of stars formed during one star formation event in an initially gravitationally-bound region in a molecular cloud (on a 1 pc scale and within about 1 Myr in a spatially and temporarily correlated star-formation event, CSFE, i.e. an embedded cluster; see Sec. 1.1.2). We refer to the *cIMF* as

4 The initial mass function of stars and the star-formation rates of galaxies

the composite-IMF, i.e. the sum of the IMFs over larger regions in a galaxy (e.g. stellar associations, cf. Vanbeveren 1982; Hopkins 2018). The *gwIMF* is the initial stellar mass function of *newly* formed stars in a whole galaxy, as observed for example with integrated-light indicators.

These abbreviations are visualised in Fig. 1.1.

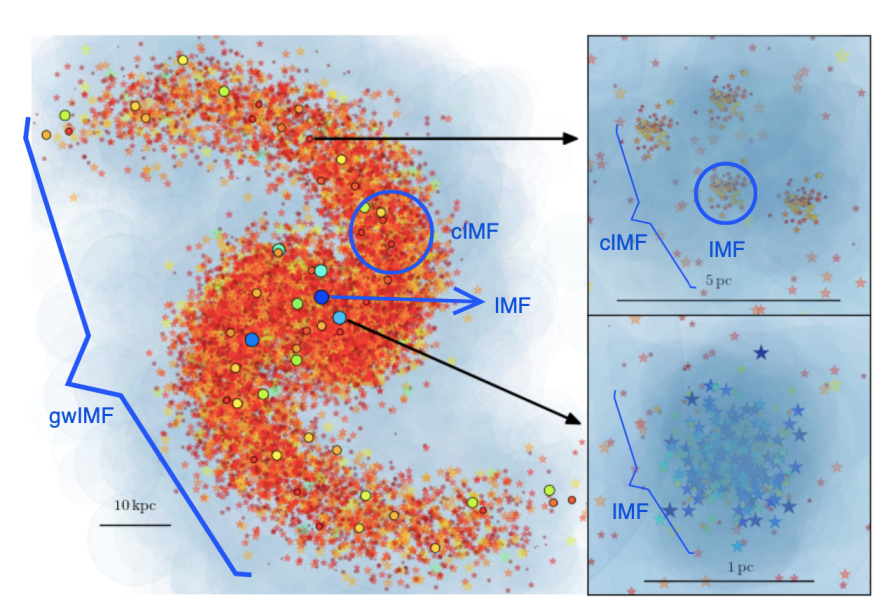


Figure 1.1 Schematic showing a late-type star forming galaxy. Its field population is represented by red and orange stars. The newly formed stellar population is marked by colored circles which represent CSFEs (embedded star clusters/ active star forming units). The colors and sizes of symbols scale with stellar and cluster mass. **Right bottom panel:** A young massive embedded cluster, which will most likely survive and contribute to the galaxy's open star cluster population (Brinkmann et al., 2017). **Right top panel:** Young embedded cluster complex composed of a number of low-mass embedded clusters (as observed e.g. in the Orion clouds by Megeath et al. 2012, 2016), which will evolve into a T-Tauri association once the embedded clusters expand after loss of their residual gas and disperse into the galaxy field stellar population (Kroupa and Bouvier, 2003; Joncour et al., 2018). Adapted from Jeřábková et al. (2018).

If we define the standard form of the IMF as the canonical IMF (e.g. Eq. 1.1), then, relative to this canonical IMF, a top-heavy IMF, cIMF or gwIMF is one which has a surplus of massive $(m \gtrsim 10~M_{\odot})$ stars, a top-light one has a deficit of massive stars and is thus also bottom-heavy, a bottom-heavy one has a surplus of low-mass ($\lesssim 0.7~M_{\odot}$) stars and a bottom-light one has a deficit of low-mass stars. But it is clearly the slope of the IMF which sets the terminology. This is visualised in Fig. 1.2

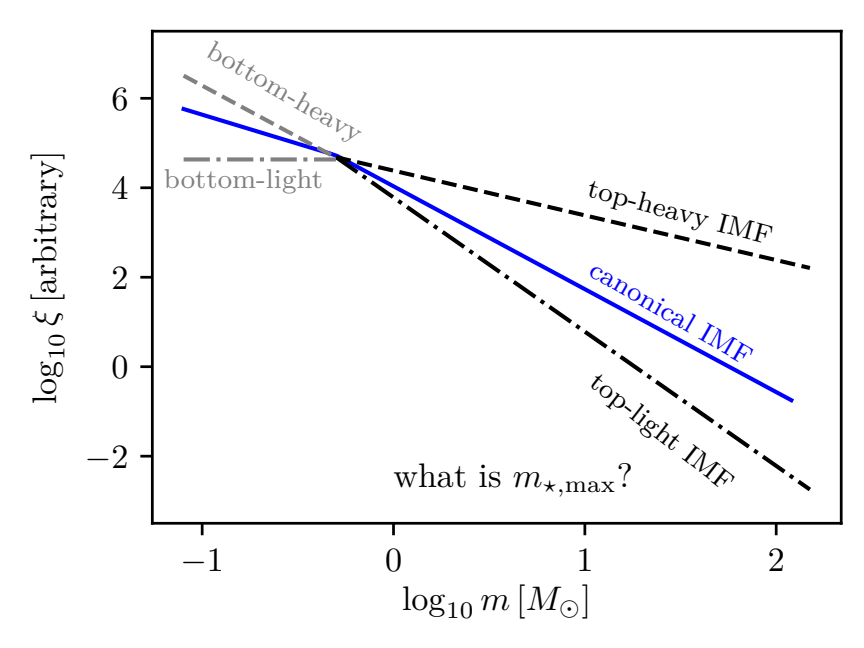


Figure 1.2 A sketch to visualise the meaning of a top-heavy, top-light, bottom-heavy and bottom-light IMF, cIMF and gwIMF. The question posed in the panel concerns whether a fundamental maximum physical stellar mass, $m_{\text{max}*}$, exists such that all born stars have initial masses $m \leq m_{\text{max}*}$.

Note that if the IMF would be a universal probability density function (PDF) then IMF=cIMF=gwIMF (Box The Composite IMF-PDF Theorem on p. 28). On the other hand, if the IMF varies and/or if it is not a PDF, then in general IMF \neq cIMF \neq gwIMF. It is therefore important to introduce this terminology and to discuss various concepts as to what the mathematical nature of the IMF may be and how this may relate to the physics of star formation, as we do in the following text.

Throughout this text we refer to the ECMF as the embedded cluster mass function, i.e. the mass distribution of freshly formed embedded clusters (Eq. 1.13 below). The same considerations as for the cIMF and the gwIMF also apply to the ECMF (cECMF and the gwECMF), but we do not discuss these here in further detail apart from mentioning that a Schechter-type form of the galaxy-wide ECMF (the gwECMF) arises naturally if the ECMF is a power-law function (Lieberz and Kroupa, 2017).

1.1.2 Turbulence, filaments, embedded clusters and associations

The problem discussed here is how the galaxy-wide IMF, which is relevant for extragalactic research, is related to the stellar IMF which is observationally deduced in individual star-formation regions within galaxies. One ansatz is to develop a theoretical galaxy-wide description of how a turbulent interstellar medium (ISM) generates the gwIMF (Hopkins, 2012). Another ansatz is to use the IMF deduced from observations of resolved stellar populations as a boundary condition in the problem, which, if successful, has the advantage that this ansatz would be automatically consistent with observations on galaxy-wide scales as well as on molecular-cloud scales.

In Fig. 1.1 the regional IMF (cIMF) and the galaxy-wide IMF (gwIMF) are visualised as arising from the IMF which is established by the star-formation process. An important issue for the discussion below is how this star-formation is arranged. Is a stochastic approach, according to which stellar masses are chosen randomly from the IMF whenever star formation occurs, a reasonable approximation? Or is a more elaborate, physically motivated calculation more appropriate?

The interstellar medium (ISM) is in a state of flow within the potential of the galaxy and comes in different physical, interrelated and constantly time evolving thermally unstable and non-equilibrium phases (Breitschwerdt et al., 2012). The complex structure of the ISM may, to a certain approximation and on a sufficiently large scale, be described as a turbulent dissipative medium (being constantly energised by rotational shear, supernova explosions, stellar winds, Breitschwerdt et al. 2012; Burkert 2006; Federrath 2016). Where the density becomes sufficiently large the gas can recombine, cool by line emission and form molecules. Observations inform us that a small fraction of the molecular phase achieves a sufficiently dense state to collapse under self-gravity to form stars. When this happens, typically much more mass is available than will end up in a late-type star, and thus small groups of stars to major clusters can form. The gas seems to loose its turbulent nature when denser and forms a complex pattern of intertwined filaments which appear to accrete gas from their environment (André et al., 2010, 2014; Federrath, 2016; Shimajiri et al., 2017).

Protostars (ages < few 10^5 yr) are observed to form in these thin ($\approx 0.1 \,\mathrm{pc}$), phase-space coherent long (> 1 pc) molecular cloud filaments with life-times of a few 10^5 yr (e.g. Hacar et al. 2013; André et al. 2014; Könyves et al. 2015; Hacar et al. 2017b,a). The filaments fragment into protostars, and compact groups of stars (we refer to these as *embedded clusters*) appear where such filaments intersect (Schneider et al., 2012; André et al., 2014).

Embedded clusters are those compact (< 1 pc) regions which are gravitationally bound (since the gas falls into them along the filaments). Examples of embedded clusters are the compact groups of stars in the Taurus star forming region referred to as Nested Elementary STructures (NESTs) by Joncour et al. (2018), the many low-mass groups of stars in the southern part of the Orion A cloud and the Orion Nebula Cluster (Megeath et al., 2016). Marks and Kroupa (2012) derive a half-mass-radius-embedded-stellar-cluster-mass relation (eq. 1.5 below), which leads to a density-mass relation consistent with (a) observed molecular cloud cores and (b) independent estimates of the initial densities of globular clusters. The time when an embedded cluster reaches r_h can be identified with t_{math} in Box The Empirical IMF Dependence on p. 26. Interesting here is that this radius—mass relation is qualitatively consistent with the dense embedded clusters that form in hydrodynamical simulations (Bate et al., 2014) and that it leads to $r_h \approx 0.1 \,\mathrm{pc}$ for $M_{\rm ecl} = 1 \, M_{\odot}$, which is the same spatial dimension as that of a filament along which late-type stars form nearly equidistantly (André et al., 2010, 2014). If the observed open clusters have gone through such a dense state, then they can expand to their present-day radii (about 3 pc) through the expulsion of residual gas assuming a star-formation efficiency of 33 % (Banerjee and Kroupa 2017, Eq. 1.4).

Numerical simulations of star formation in molecular clouds as well as Nbody simulations of realistic (i.e. including a high primordial binary proportion and stellar evolution) embedded clusters prove these to be dynamically active (Bate, 2005, 2014; Bate et al., 2014), whereby the rate and energy of the activity (ejections of stars and binaries) is small in NESTs (Kroupa and Bouvier, 2003) and dramatic in clusters containing thousands of stars (Oh et al., 2015; Oh and Kroupa, 2016). Thus, stars are ejected from the star-forming embedded clusters due to the encounters between stars and due to the high multiplicity fraction. An embedded cluster rapidly (within a few 10^5 yr) populates the region (> few \times 10 pc) around it with stars and binaries moving away from it. These may be identified as being part of a distributed population. The discussion of a distributed versus clustered mode of star formation (Gieles et al., 2012), based on the observed distribution of very young stars (ages $\lesssim 1 \,\mathrm{Myr}$), needs to take this into account. This is an important issue in the consideration of the gwIMF and how it is related to the star-formation process in a galaxy (a purely distributed mode would, for example, be consistent with a PDF interpretation of the IMF).

Given that "clusters" are ill defined in this context, we note that the protostars in the filaments can be mathematically treated as being the low-density outer region of the embedded clusters. Thus, for example, the Plummer .

model (Plummer 1911; the simplest solution of the collision-less Boltzmann equation, Heggie and Hut 2003; Kroupa 2008, and a good representation of observed clusters) always has individual members beyond a few Plummer radii which may, depending on the chosen definition of cluster membership, be defined to be part of an isolated or distributed population. For practical purposes, and also in good approximation to the observation that the great majority of protostars are found by surveys to be in embedded clusters (Lada and Lada, 2003; Lada, 2010), we can assume, as one possible hypothesis, that embedded clusters are the fundamental units of star formation (Kroupa, 2005). This hypothesis is supported by theoretical studies of the turbulent ISM in galaxies (Hopkins, 2013b) and is useful because it allows us to identify an IMF with an embedded cluster. It is not the sole hypothesis though to be investigated, as we discuss below.

For completeness, in view of the discussion of how OB and T-Tauri associations form, an understanding can be formulated according to which a density wave in a spiral galaxy sources a minimum potential wave in which the in-falling in-homogeneous ISM condenses as molecular clouds (Fukui and Kawamura 2010; Heyer and Dame 2015; in a sense like bad-weather regions). Stars form in these and move out of the potential minimum along with the molecularised ISM. The molecular clouds thus disperse most likely by themselves just behind the potential minimum wave but also helped by the feedback from the freshly formed stars. Each molecular cloud typically spawns a number of embedded clusters which expand once the stars expel the residual gas, whereby their expansion rate depends on the mass of an embedded cluster (slow for low-mass cases; Brinkmann et al. 2017). Evidence for a complex kinematical field of young stars in associations has been reported (Wright and Mamajek, 2018). Thus, in this view, a stellar association is always present on the other side of the potential minimum wave as long as the ISM flows relative to the spiral pattern (Egusa et al., 2004, 2009, 2017). This association may be contracting or expanding and may also selfregulate and stimulate further star-formation (Lim et al., 2018), depending on the details of the ISM flow through the potential wave.

Independently of whether embedded clusters may be the fundamental units of star formation, the few-pc long, 0.1 pc wide filaments though cannot exist in a turbulent medium, since it implies that the velocity differences between regions grow randomly with spatial scale such that the filaments cannot be phase-space coherent over scales of more than a pc (on scales longer than the smallest turbulence length-scale). It is thus the decay of the turbulent-like phase which allows the filaments to form.

At the point in time when the stars begin to form, the gas therefore cannot be described as being a turbulent medium.

An important problem thus arises: is the process of star formation (which yields the IMF) given by gravo-thermal-turbulence according to which the molecular cloud is in a state of turbulence which determines the density peaks which collapse under self-gravity to form stars (Padoan and Nordlund, 2002; Hennebelle and Chabrier, 2013; Hopkins, 2013a; Haugbølle et al., 2018)? This theoretical approach requires constant energy input into the cloud on all scales in order to retain the turbulence. But self-consistent computations of turbulent clouds cast doubt on turbulent fragmentation explaining the IMF as low-mass proto-stars tend to be destroyed through shocks before they can form (Bertelli Motta et al., 2016; Liptai et al., 2017). On the other hand, the IMF might be related to the fragmentation of filaments instead (e.g. André et al. 2010, 2014; Shimajiri et al. 2017). That is, the IMF may not be determined by the PDF given by the turbulent molecular cloud, but rather by fragmentation of the dense filaments.

1.2 Can the IMF be measured?

Even if dust obscuration and reddening were not to matter, the IMF does not exist as a real distribution function of initial stellar masses because the time does not exist when all the stars formed together would be found in a star-forming region. The reasons for the non-existence of the IMF in nature are: (i) while the most massive stars are already evolving off the main sequence having a substantial mass loss, some of the low mass stars may not have been formed fully yet in the star-forming event; (ii) stars are ejected even before the embedded cluster is finished forming (e.g. Kroupa et al. 2018; Wang et al. 2019), stellar mergers occur (de Mink et al., 2014; Oh and Kroupa, 2018) and (iii) expulsion of residual gas unbinds low mass stars from the very young cluster within a crossing time if clusters form mass segregated (Haghi et al., 2015).

Something which does not exist can also not be measured ("The IMF Unmeasurabilty Theorem" of Kroupa et al. 2013). But the IMF can be deduced from observations as a mathematical hilfskonstrukt (Kroupa and Jerabkova, 2018), to allow calculations and modelling of stellar populations. But in order to do so statistical corrections are necessary to account for the time evolving binary population in the embedded and exposed cluster (Belloni et al., 2017, 2018), loss of stars through ejections (Banerjee and Kroupa, 2012; Oh et al., 2015; Oh and Kroupa, 2016), mergers and gas expulsion,

as well as the corrections for the changes in stellar mass through stellar and binary evolution (Sana et al., 2012; Schneider et al., 2015) and energy-equipartition-driven stellar-dynamical evolution (Baumgardt and Makino, 2003; Baumgardt et al., 2008).

THE EXISTENCE OF THE IMF:

The IMF is a mathematical hilfskonstrukt which does not have a physical representation, but which is needed for initialising stellar populations.

This is a reasonable description because the early evolutionary processes mentioned above take part largely on short time scales (e.g. the formation of the stellar population in an embedded cluster takes not longer than about one Myr) such that when studying stellar populations on longer time-scales the non-physical nature of the IMF can be neglected. It is therefore possible to obtain an estimate of the complete sample of stars that formed together and to quantify their birth masses in order to construct the IMF as if this IMF were to represent a complete population of all the stars formed together at exactly the same time, for example in one embedded cluster (Sec. 1.1.2). When doing so for a pre-main sequence population, the flux observed from a young star needs to be converted to a mass, and this calculation needs to be done using pre-main sequence stellar evolutionary tracks which are increasingly uncertain for younger ages (Wuchterl and Tscharnuter, 2003).

But it should be clear that the concept of an IMF fails when considering the first Myr of a stellar population.

1.3 What is the shape of the IMF?

The most direct approach to quantify the shape of the IMF is to use resolved stellar populations and these are, by necessity, mostly restricted to the Galaxy.

One important ansatz to assess the shape of the IMF is to measure a representative and complete sample of stars near to the Sun and to calculate their birth masses to construct this Galactic-field average IMF (and to implicitly assume this composite IMF of the Solar neighbourhood to be the IMF). This approach has been followed by many teams and entails two general procedures (the reviews are listed in Section 1.1) to assess the IMF for stars with $m \lesssim 1\,M_\odot$: (i) counting stars in a complete volume near to the Sun and (ii) taking pencil beam surveys through the Galactic disk. Approach (i) has the advantage that the stars are close-by allowing their multiplicity to be better assessed and that trigonometric parallax measurements yield stellar distances directly. But the disadvantage is that the census of

very low-mass stars becomes incomplete beyond about 5-10 pc distance from us (Scalo, 1986; Henry et al., 2018; Riedel et al., 2018). Approach (ii) has the advantage that the stellar census is significantly enlarged even at very low masses because telescope-integration times can be chosen to be long per field, but the disadvantage is that distances need to be inferred using photometric parallax and that companions in multiple stellar systems are likely not detected (Kroupa, 1995c). In the course of this research the shape of the late-type stellar luminosity function was discovered to be universal and largely given by the stellar mass-luminosity relation, and unresolved binaries to play a significant role in establishing the difference between star counts under (i) and (ii). A completely independent approach to the above star-count ones is to use microlensing time scales to assess the distribution of lensing masses. This yields constraints on the IMF deducible from mainsequence-field stars in the inner Galaxy which are well-consistent with those obtained from the star-counts under approaches i and ii (Wegg et al., 2017). This overall research effort has thus lead to the gwIMF of the Galactic thin disk being now constrained quite well. This Galactic-field average IMF (i.e., the gwIMF as constructed from the local Solar neighbourhood field) can be conveniently written as a three-part power-law form with $\alpha_1 \approx 1.3 \pm 0.3$ for $0.07 \lesssim m/M_{\odot} < 0.5$, $\alpha_2 \approx 2.3 \pm 0.3$ for $0.5 < m/M_{\odot} \le 1$ and α_3 for $m > 1 M_{\odot}$ (Eq. 4.59 in Kroupa et al. 2013).

The constraints for $m \gtrsim 1 M_{\odot}$ still stem largely from the analysis by Scalo (1986). This monumental work explains in detail how the $m < 1 M_{\odot}$ and the $m > 1 M_{\odot}$ star counts need to be combined since the stellar life-times and thus their distributions in the Galactic thin disk differ greatly and are subject to changes in the SFR (Elmegreen and Scalo, 2006). Assuming the Galactic-field IMF to be continuous across $m \approx 1-10 M_{\odot}$, it comes out that it is rather steep for $m \gtrsim 1 M_{\odot}$, with $\alpha_3 = 2.7 \pm 0.4$ being an approximative summary (Eq. 4.59 in Kroupa et al. 2013). Such a steep Galactic-field IMF deduced from the wider (kpc-scale) Solar-neighbourhood star-counts has been more recently constrained by Mor et al. (2017, 2018) using the Besançon Galaxy Model fast approximate simulations technique, which combines photometric data with a spatial and kinematical model of the Galaxy yielding $\alpha_3 = 2.9^{+0.2}_{-0.2}$ and $\alpha_3 = 3.7^{+0.2}_{-0.2}$ depending on the used extinction map, with an increasing uncertainty for $m > 4 M_{\odot}$ due to the extreme rarity of such stars. This steep index is also found by Rybizki and Just (2015) using their forward modelling method, which also combines kinematical and photometric data with a model of the Milky Way. We note though that a single power-law description for $m > 1 M_{\odot}$ is only a very rough approximation since the field-IMF, as reconstructed from the star-counts, is curved

and this curvature contains information on the competition of the rates with which stars were and are being born and are dying (Elmegreen and Scalo, 2006) as well as on the individual star-formation events which combine to make the Galactic-field IMF (Zonoozi et al. 2019, see also Fig. 1.5 below).

The other major approach to assess the shape of the IMF is to target individual star clusters and/or OB associations in an attempt to infer the IMF within these. The advantage is that the stars have very nearly the same age, metallicity and distance. The problem is that the early and secular dynamical evolution of the clusters leads to a significant time-dependent change in the shape of the stellar mass function through very early stellar ejections, stellar evaporation (which depends on the time-evolution of the tidal field), break-up of binary systems over time as well as the odd stellar merger occurring (see Sec. 1.4 above for more details).

As outlined in the reviews mentioned above, the general finding is that the IMFs reconstructed from the observed populations are consistent with the canonical IMF (Eq. 1.1). Until recently there has not been a significant evidence for a variation of the IMF within the star-formation events in the Milky Way (but see Sec. 1.5) and the notion that the IMF equals the composite Galactic-field IMF (from the Solar neighbourhood ensemble of stars) was affirmed for stars with $m \lesssim 1 \, M_{\odot}$.

The Canonical IMF: (m is in units of M_{\odot} , k is the normalisation constant)

$$\xi_{\text{BD}}(m) = \frac{k}{3} \left(\frac{m}{0.07}\right)^{-0.3 \pm 0.4}$$
 , $0.01 < m \lesssim 0.15$

$$\xi_{\text{star}}(m) = k \left\{ \begin{bmatrix} \left(\frac{m}{0.07}\right)^{-1.3 \pm 0.3} & , & 0.07 < m \le 0.5, \\ \left[\left(\frac{0.5}{0.07}\right)^{-1.3 \pm 0.3}\right] \left(\frac{m}{0.5}\right)^{-2.3 \pm 0.36} & , & 0.5 < m \le 150. \end{bmatrix} \right.$$
(1.1)

We note that the canonical IMF may be either described as a two-part-power-law function (Eq. 1.1 above, Eq. 4.55 in Kroupa et al. 2013) or a lognormal form (between the hydrogen burning mass limit, $m_{\rm L}\approx 0.07\,M_{\odot}$, and about $1\,M_{\odot}$) with a power-law extension above $\approx 1\,M_{\odot}$ (Eq. 4.56 in Kroupa et al. 2013). The former (Eq. 1.1) is convenient for use in computations and is adopted throughout this work. It can also be written as a multipower-law form ($\propto m^{-\alpha_i}$) with $\alpha_1\approx 1.3\pm 0.3$ for $0.7\lesssim m/M_{\odot}<0.5$, $\alpha_2\approx 2.3\pm 0.3$ for $0.5\leq m/M_{\odot}\leq 1$ and $\alpha_3=\alpha_2$ for $m>1\,M_{\odot}$ (Jeřábková et al., 2018). The canonical log-normal+power-law form is indistinguishable from the canonical two-part-power-law form.

But as already reported above, for more-massive stars, the field-star-counts consistently yield steeper IMFs than the canonical IMF. This difference in α_3 as obtained from individual embedded or young clusters on the one hand side, and from the Galactic-field star counts, which are a result from the combination of many star-formation events on the other hand side, provides an important hint as to how the composite IMF (i.e. cIMF) emerges from the star-formation events in a galaxy (Kroupa and Weidner 2003; Zonoozi et al. 2019, see Sec. 1.6.2). The bar region of the inner Galaxy has been found to be consistent with the canonical IMF using Made to Measure and chemodynamical modelling (Portail et al., 2017), while there are some indications that the Galactic bulge may have formed with a top-heavy IMF in order to account for the metal-rich stars (Ballero et al., 2007).

Brown dwarfs (BDs) are not discussed here. They add negligible mass and are a by-product of star formation following their own IMF (as planets follow their own IMF, see Eq. 4.55 in Kroupa et al. 2013) and binary pairing rules different to those of stars and typically they do not pair with stars (Bate et al., 2002; Thies et al., 2015). The microlensing constraints from the inner Galaxy are consistent with these results (Wegg et al., 2017). Note that in Eq. 1.1 the BD IMF overlaps with the stellar IMF which comes about due to the star-like and BD-like formation processes overlapping (Thies et al., 2015).

1.4 What is the mathematical nature of the IMF?

From a complete co-eval ensemble of stars an IMF can be constructed, and thus this IMF is a description of the distribution of initial stellar masses. The physics of star formation determines the form of the IMF, but it also determines which type of distribution function the IMF is.

A turbulent-fragmentation process (Sec. 1.1.2) might imply the IMF to be a probability distribution (PDF) function. A self-regulated growth process might instead imply the IMF to be an optimal distribution function (ODF), such that the distribution of stellar masses actually formed does not have Poisson scatter (Kroupa et al., 2013). Nature may well be in-between both extremes. For example, it may be probabilistic to some degree (the butterfly effect: two identical gas clouds which differ in some property by an infinitesimal amount lead to two IMFs, the distance between which is, in some metric, related to the Poisson uncertainty given by the number of stars formed). Or it may be deterministic in the sense that the bulk properties of the cloud (its temperature, density and chemical composition) determine the shape of the distribution function. But if the butterfly effect is minor, because the

system is highly self-regulated and insensitive to small differences in initial conditions, or because any physical state of the inter-stellar medium decays to a universal filamentary structure, then the ODF description may be more appropriate.

A major aspect of IMF research is thus not only to find the form of the IMF and its possible variation, but also to understand which type of distribution function we are dealing with. This is important for initialising stellar populations in galaxies and the mathematical methods how to do so differ significantly: random vs optimal sampling (Kroupa et al., 2013; Schulz et al., 2015; Applebaum et al., 2020).

MATHEMATICAL NATURE OF THE IMF:

There are thus two main hypotheses as to the mathematical nature of the IMF: it is a PDF or an ODF. Each hypothesis can be tested against data to infer the valid nature that may lie between these two extreme descriptions.

1.4.1 The IMF as a PDF

An often-used interpretation is the IMF to be a PDF (e.g. Elmegreen 1997; Kroupa 2001; Cerviño et al. 2013a,b): when stars form in some system, their masses appear randomly within the system, subject to being drawn from the IMF. This is the stochastic, or probabilistic, description of star formation within a galaxy. That is, the probability of finding a star of mass m in the interval m_1 to m_2 is

$$X_{12} = \int_{m_1}^{m_2} \xi_{\rm p}(m) \, dm, \tag{1.2}$$

where $0 \le X_{12} \le 1$ is uniformly distributed and $X_{12} = 1$ for $m_1 \approx 0.07 M_{\odot}$ (the lower-mass limit, $m_{\rm L}$) and $m_2 = m_{\rm max}$ which is some upper limit which may be infinite or have a physical limit. Note also that the probability density distribution function is proportional to the IMF,

$$\xi_{\rm p}(m) \propto \xi(m),$$
 (1.3)

such that the integral from $m_{\rm L}$ to $m_{\rm max*}$ over the former yields 1 while over the latter it yields the number of stars in the population.

If the IMF is a PDF then any observation of a co-eval stellar population will be subject to Poisson-differences such that a measured IMF for population A will differ from that measured for population B, with the difference, $\xi_{\rm A}(m) \, dm - \xi_{\rm B}(m) \, dm$, being consistent with Poisson scatter for the sizes of the populations (assuming no observational errors and all individual stars to be observed). It is thus of much fundamental interest to search if such

variations are observed (Elmegreen, 1999; Kroupa, 2001; Elmegreen, 2004; Dib, 2014; Ashworth et al., 2017).

A prominent test of the hypothesis that the IMF is an unconstrained (scale-free) PDF is to consider the masses of the most massive stars observed (Box Observational Constraints I on p. 16). We would expect to see stars weighing a few $1000\,M_\odot$ in populous galaxies (Elmegreen, 2000). But the observed most massive stars have $m\approx 300\,M_\odot$ (Crowther et al., 2010; Schneider et al., 2014). This suggests that the IMF may be a PDF but with the constraint $m_{\rm max*}\lesssim 300\,M_\odot$ (more on this in the Box Observational Constraints I on p. 16).

It is possible to deduce that the stellar IMF varies without specifying a possible systematic variation with some physical property of the star-forming environment (Dib, 2014; Dib et al., 2017). But by taking account of all of the relevant biases, survey differences, observational uncertainties and also additional effects such as arising from patchy reddening in star-forming regions and, importantly, the very large uncertainties in calculating stellar masses from the observed fluxes for pre-main sequence stars (Wuchterl and Tscharnuter, 2003), the general consensus has been reached that the IMF is invariant, at least for the stellar populations probed in the Milky Way (Kroupa, 2002a; Chabrier, 2003; Bastian et al., 2010; Kroupa et al., 2013; Offner et al., 2014). More technically, the hypothesis that the IMF is invariant and canonical cannot be discarded with sufficient confidence, the variation of the IMF shape being found to be too small even compared to the expected Poisson scatter (Box Observational Constraints I on p. 16).

The notion also emerged in the literature that massive stars can form in isolation. Finding undisputed such cases would constitute a strong argument for the IMF being a PDF and for a stochastic description of star formation (Box Observational Constraints I on p. 16). Interesting is that the cases of presumed isolated massive star formation in the Milky Way, the Large and Small-Magellanic clouds have successively been shown to be untenable when improved observational data became available, and that meanwhile ever distant dwarf galaxies, such as the Sextans A dwarf galaxy at about 1.3 Mpc, are now heralded as such cases in-proof (Garcia et al., 2019). If it were true that star formation is stochastic, then the observationally deduced power-law indices of the IMF, α_i , would vary according to the Poisson dispersion (even if the parent IMF were invariant, e.g. Kroupa 2001), since some O stars may be isolated, others would be in rare clusters with a deficit of low mass stars while other populous clusters would not have any O stars.

OBSERVATIONAL CONSTRAINTS I: This box lists some key observations relevant for testing the conjecture that the IMF is a PDF.

- The most massive stars weigh $m_{\text{max*}} \approx 150\,M_{\odot}$ (Weidner and Kroupa, 2004; Figer, 2005; Oey and Clarke, 2005; Koen, 2006; Maíz Apellániz et al., 2007). Crowther et al. (2010); Schneider et al. (2014) find evidence for the existence of $m \approx 300\,M_{\odot}$ stars. These are consistent with $m_{\text{max*}} \approx 150\,M_{\odot}$ as a result of mergers in their dense massive birth clusters (Banerjee et al., 2012), but further study is needed to ascertain if the observed number of such super-canonical stars can be obtained through mergers and binary-star evolution in dense starburst clusters (cf. Oh and Kroupa 2018).
- The small dispersion of observationally derived IMF power-law indices (which contain all the uncertainties and come from different teams with different observational procedures), $\alpha_3 = 2.36 \pm 0.08$, above $2.5\,M_{\odot}$, compared to models which have no observational uncertainties but which include binaries, stellar dynamical processes and assume the IMF to be a PDF ($\alpha_3 = 2.20 \pm 0.63$), suggest the IMF to be remarkably invariant, the different populations showing differences in the IMF which are smaller than the expected Poisson scatter if the IMF were a PDF (Kroupa, 2002a).
- Most early-type stars supposed to have formed in isolation have been found to be propagating from some young cluster (Gvaramadze et al., 2012), be in hitherto unknown compact clusters (Stephens et al., 2017) or be explainable through the two-step ejection process (Pflamm-Altenburg and Kroupa, 2010).
- Hsu et al. (2012) observe in the Orion A cloud that the very young stellar populations formed in low-mass embedded clusters in its southern part significantly lack massive stars although statistically the same total number of stars (a few thousand) have formed as in the Orion Nebula Cluster in the northern part of the same cloud. If the IMF were to be a PDF, then both ensembles ought to have the same number of massive stars within the statistical uncertainties. Thus the IMF seems to differ in the two regions and massive stars appear to correlate with the mass in stars of the embedded clusters.
- Kirk and Myers (2011, 2012) find, in their homogeneous survey of very young clusters, a pronounced correlation of the mass of the most massive star, m_{max} , with the stellar mass of the embedded cluster,

- M_{ecl} , for low mass systems (the data lie near the $m_{\text{max}} = WK(M_{\text{ecl}})$ relation, see the next point).
- Stephens et al. (2017) performed a high resolution survey of previously thought isolated massive stars in the LMC in order to test their isolated nature. They found each of them to be contained in a compact massive stellar cluster of 1-3 Myr age. The $m_{\rm max}$ and $M_{\rm ecl}$ values are correlated (the data lie near the $m_{\rm max} = WK(M_{\rm ecl})$ relation, see the next point).
- Ramírez Alegría et al. (2016) find a correlation of the most-massive star with the cluster mass in the sample of VVV-survey young (< 10 Myr old) clusters.
- Weidner and Kroupa (2006); Weidner et al. (2010, 2013c) collate data on very young clusters from the literature, selecting the clusters to be pre-supernova age (< 4 Myr age being the only selection criterion) avoiding loss of stars through supernova explosions, and significantly limiting dynamical and stellar evolution affects. They find m_{max} to significantly correlate with $M_{\rm ecl}$, the dispersion of $m_{\rm max}$ values being largely consistent with the observational uncertainties such that intrinsic scatter appears to be small. They calculate that the hypothesis that the IMF is a PDF is consistent with the data at the 0.1 % confidence level. The possible existence of a physical $m_{\text{max}} = WK(M_{\text{ecl}})$ relation is discussed (Fig. 1.3, see also fig. 1 in Yan et al. 2017, which compare all above data by Kirk and Myers 2011, 2012; Weidner et al. 2013c; Ramírez Alegría et al. 2016; Stephens et al. 2017). It may be a consequence of a feedback-self-regulated growth process of stellar masses. Noteworthy is that the APEX/SABOCA survey of starforming molecular cloud clumps by Lin et al. (2019) shows a similar correlation to exist between the most massive core mass and the proto-cluster clump mass (Fig. 1.3). The flattening of this to the stellar relation above $m_{\rm max} \approx 10 \, M_{\odot}$ may be due to resolution limiting the identification of less-massive sub-clumps in the former, additional fragmentation in the former and feedback self-regulation during the transformation of the proto-stellar clump to a star (Beuther et al., 2007; Zinnecker and Yorke, 2007).
- Deviations from an assumed $m_{\text{max}} = WK(M_{\text{ecl}})$ relation, reported by e.g. Chené et al. (2015), can be understood naturally as arising from stellar mergers and ejections in and from embedded clusters (Oh and Kroupa, 2012, 2018).
- Observed very young embedded clusters (not older than a crossing

time) have been found to be mass segregated (Bontemps et al., 2010; Kirk et al., 2014; Lane et al., 2016; Kirk et al., 2016; Plunkett et al., 2018). The ALMA data by Plunkett et al. (2018) are interesting, as they suggest that a proto-cluster is forming perfectly mass segregated (Pavlík et al., 2019). If this were to be the case then this suggests a high degree of regulation during the star-formation process with the individual stellar masses being a sensitive function of the core-density and thus gas reservoir (which varies radially in the embedded cluster), which most probably defines the accretion rate (Bonnell and Davies, 1998). Noteworthy is that this consideration appears to be consistent with the possible existence of a physical $m_{\text{max}} = WK(M_{\text{ecl}})$ relation noted above. Nbody models of the Orion Nebula Cluster (< 2.5 Myr old) also indicate it to be primordially mass segregated (Bonnell and Davies, 1998). Observationally, data on globular clusters also suggest them to have been born mass segregated (Baumgardt et al., 2008; Haghi et al., 2015). If the IMF were a PDF then the stellar mass drawn randomly from the IMF ought not to correlate with the position of the star.

Given the collation in Box Observational Constraints I (p. 16), can the IMF still be a PDF on an embedded cluster scale? One particular observational challenge addresses this question: a physical $m_{\text{max}} = WK(M_{\text{ecl}})$ relation should not exist and the $m_{\text{max}}, M_{\text{ecl}}$ data should be consistent with randomly drawing stars from the IMF if it is a PDF. Prior to the more recent observational surveys by Kirk and Myers (2011, 2012), Ramírez Alegría et al. (2016) and Stephens et al. (2017) mentioned in Box I (p. 16), Parker and Goodwin (2007); Maschberger and Clarke (2008); Cerviño et al. (2013a) addressed this problem using their own star-by-star data collations and statistical analysis negating that the relation exists. Andrews et al. (2013, 2014) also addressed this problem based on unresolved young star clusters in dwarf galaxies using broad-band photometry, spectral-energy-density (SED) modelling and H α flux measurements to conclude that this relation does not exist, therewith formulating a strong conclusion at 1σ significance. Being part of this team, this conclusion is echoed in the review by Krumholz (2014). For completeness, it is noted here that Weidner et al. (2014) showed these same extragalactic data to be well consistent (within 1σ uncertainty) with the existence of a physical $m_{\text{max}} = WK(M_{\text{ecl}})$ relation, largely because the random sampling in connection with m_{max} being assumed to be a truncation limit was applied incorrectly in these and other publications (e.g. Fumagalli et al. 2011, also part of the Krumholz effort), noting also that field-star con-

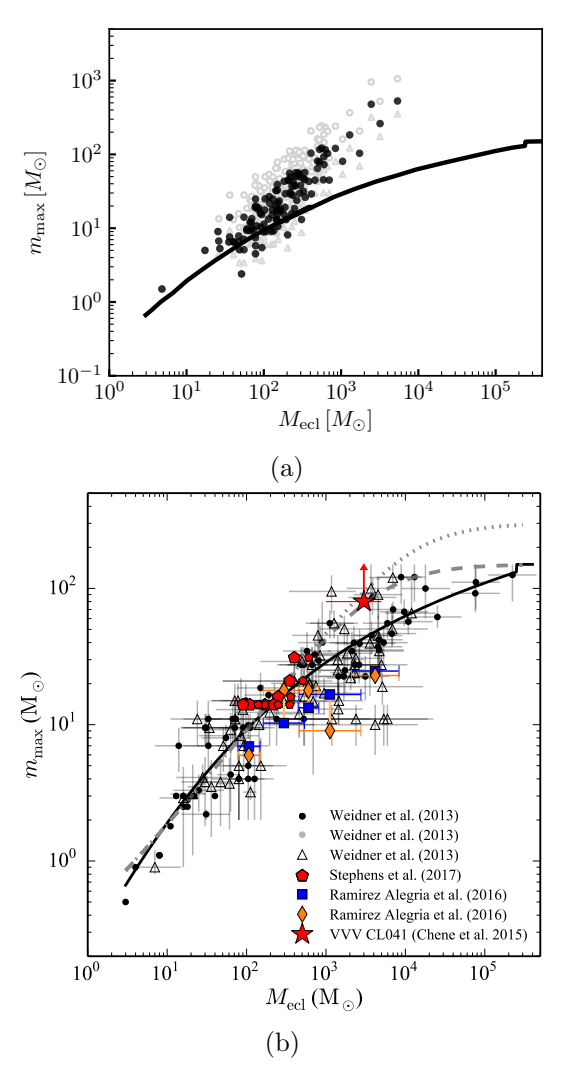


Figure 1.3 Panel a: Data from the Lin et al. (2019) APEX/SABOCA survey of star-forming molecular cloud clumps. The measured most-massive sub-clumps with masses $m_{\rm scl} = m_{\rm max}/\epsilon$ are plotted as grey open circles in dependence of their hosting measured proto-cluster of molecular-gas mass $M_{\rm pcl} = M_{\rm ecl}/\epsilon$ assuming each proto cluster and clump has a star formation efficiency of $\epsilon = 1/3$. The black circles assume each $m_{\rm max} > 10 \, M_{\odot}$ value fragments into two equal mass sub-cores and the open triangles assume fragmentation into three sub-cores. Panel b: The $m_{\rm max}, M_{\rm ecl}$ stellar data and the $m_{\text{max}} = WK(M_{\text{ecl}})$ relation (eq. 1 in Weidner et al. 2013c depicted as the black solid line, shown also in panel a). The black circles are the small-error sub-sample data in the < 4 Myr old clusters used to obtain this relation. The open triangles have large uncertainties and are excluded from the fit. The red star is VVV CL041 put forward by Chené et al. (2015) as not fitting the $m_{\text{max}} = WK(M_{\text{ecl}})$ relation. Oh and Kroupa (2018) explain such deviant cases as being produced through mergers in the young compact embedded host cluster. The blue squares and orange diamonds are two different m_{max} estimates from the survey of $< 10 \,\text{Myr}$ old clusters by Ramírez Alegría et al. (2016) and the red pentagons (large for 1 Myr age and small for 2.5 Myr age) are the data from Stephens et al. (2017). Note how the older objects (blue squares and orange diamonds) lie below the $m_{\text{max}} = WK(M_{\text{ecl}})$ relation, consistent with stellar evolution having removed the most massive stars. The dashed and dotted lines are the semi-analytical relation (Eq. 1.6 and 1.7, from Weidner and Kroupa 2006) assuming $m_{\text{max}*} = 150 \, M_{\odot}$ and $300 \, M_{\odot}$, respectively. Adapted from Oh and Kroupa (2018).

tamination in the unresolved observations plays a role in randomising any SED.

Thus, for the time being we conclude that the existence of a physical $m_{\text{max}} = WK(M_{\text{ecl}})$ relation needs to be studied further but with great care, and we emphasise that if it were to exist then the implications for the gwIMF are major (Sec. 1.6.2).

1.4.2 The IMF as an ODF

Independently of the possibility that a physical $m_{\rm max} = WK(M_{\rm ecl})$ relation may or may not exist (Sec. 1.4.1), the observed degree of mass segregation in extremely young embedded clusters may also be seen as an indicator that a star's mass might not be random, but that it instead may be governed by the properties (mostly the density) of the molecular cloud core and thus gas reservoir within which it forms and from which it accretes. The IMF may therefore be sensitively dependent on the physical conditions within the embedded cluster. An interpretation of the IMF as an ODF may thus be a useful consideration.

If the mathematical nature of the IMF is to be understood in terms of an optimal distribution function, then how is such a description to look like? The data (Box Observational Constraints I on p. 16) suggest that $m_{\rm max}$ is determined by $M_{\rm ecl}$. If the star-formation efficiency of embedded cluster-forming cloud cores,

$$\epsilon = \frac{M_{\rm ecl}}{M_{\rm ecl} + M_{\rm gas}},\tag{1.4}$$

is typically in the range 0.1-0.3 (Megeath et al., 2016) then this dependency may arise if stars form through self-regulated accretion (on a timescale of 10^5 yr, Wuchterl and Tscharnuter 2003; Duarte-Cabral et al. 2013; Kristensen and Dunham 2018) and a link between $m_{\rm max}$ and the total embedded-cluster forming cloud core can be made. It becomes a density dependency if the birth half-mass radii, $r_{\rm h}$, of the embedded clusters are known¹

$$r_{\rm h}/{\rm pc} = 0.1 \ (M_{\rm ecl}/M_{\odot})^{0.13} \,.$$
 (1.5)

Concerning optimal sampling from the IMF, only the mass of the stellar population formed together in one star-formation event, i.e. an embedded

¹ This half-mass-radius-embedded-stellar-cluster-mass relation is derived by Marks and Kroupa (2012) from the observed binary population in open and very young clusters and assuming the truncation of the binary-binding energy distribution at low values to be a measure of the densest evolution phase of the cluster. It constitutes a theoretical approximation to the initial state of an embedded cluster for Nbody modelling.

cluster, is then relevant. A relation between m_{max} and M_{ecl} is obtained from the following two equations

$$1 = \int_{m_{\text{max}}}^{m_{\text{max}}} \xi(m) \, dm, \tag{1.6}$$

with

$$M_{\rm ecl} - m_{\rm max}(M_{\rm ecl}) = \int_{m_{\rm L}}^{m_{\rm max}} m \, \xi(m) \, dm,$$
 (1.7)

which allow solution for the two unknowns, $m_{\rm max}$ and the normalisation constant k, for the population which has the physical upper mass limit $m_{\rm max*}$ (Box Observational Constraints I on p. 16). Both equations are valid also if the IMF is a PDF and in this case $m_{\rm max}$ will be the average most massive star in an ensemble of embedded clusters (Kroupa and Weidner, 2003; Oey and Clarke, 2005). But the small dispersion of observed $m_{\rm max}$ values does not support this interpretation, as stated above in Box I.

If, on the other hand, the IMF is an ODF, then Eq. 1.6–1.7 lead directly to a good representation of the empirical $m_{\rm max}, M_{\rm ecl}$ data (dotted and dashed lines in Fig. 1.3, Weidner et al. 2013c). In order to ensure a small or negligible scatter of the $m_{\rm max}$ values, ordered sampling has been invented (Weidner and Kroupa, 2006), according to which $M_{\rm ecl}$ is iteratively solved for with increasing number of stars to minimise the difference to the observed $m_{\text{max}} = \text{WK}(M_{\text{ecl}})$ function. A more elegant method to efficiently sample stars from the IMF such that this function is obeyed is given by optimal sampling (Kroupa et al., 2013; Schulz et al., 2015; Yan et al., 2017). In optimal sampling (for an improved algorithm see Schulz et al. 2015), starting with a given $M_{\rm ecl}$ and thus $m_{\rm max}$, a sequence of stellar masses is generated step by step such that a given $M_{\rm ecl}$ has always exactly the same sequence of stars. This latter procedure is possible for whichever function $m_{\text{max}} = \text{WK}(M_{\text{ecl}})$ is adopted. One possibility is given by solving Eqs 1.6 and 1.7, but physically-motivated functions may also be used (e.g. Weidner et al. 2010 find evidence for a possible flattening of $WK(M_{ecl})$ which may be due to feedback regulation in the formation of $m_{\text{max}} \gtrsim 25 \, M_{\odot}$ stars).

An optimally-sampled stellar population has no Poisson scatter and thus fulfils two important requirements: it is consistent with the observed small dispersion of α_3 values noted above in Box I (p. 16) and it is consistent with the small dispersion of observed m_{max} values.² Dynamically stable perfectly

² Approaches which adopt the $m_{\rm max}={\rm WK}(M_{\rm ecl})$ relation but sample stars randomly from the IMF (i.e. which interpret it to be a constrained PDF) would lead to, on average, too small $m_{\rm max}$ values for each $M_{\rm ecl}$ such that the respective authors are led to erroneously conclude the WK-relation to be excluded, given unresolved data (e.g. Andrews et al. 2013, 2014). These analysis-shortcomings are elaborated on by Weidner et al. (2014).

mass-segregated embedded clusters can then be constructed readily using the methods introduced in Bonn by Šubr et al. (2008); Baumgardt et al. (2008), in order to fulfil the observational constraint that very young embedded clusters are mass segregated. These methods assume the stellar masses to be radially arranged according to their binding energy.

Summarising, the observational evidence suggests:

The IMF may be an ODF rather than a PDF.

But more research is needed to further test this assertion.

1.4.3 Emergence of apparent stochasticity

On stating the above, we note the following: Once a perfect (or highly constrained) system of stars is generated (or born), it will evolve towards what appears to be a stochastic version of itself. This follows from the second law of thermodynamics and comes about naturally because stars are ejected, binaries dissolve and stars merge and age. The Nbody computations of Oh et al. (2015); Oh and Kroupa (2016) show a large dynamical activity with the very young binary-rich clusters spurting out stars of all masses within fractions of a Myr.³

A molecular cloud which forms all its stars in a population of embedded clusters with different masses over a few Myr will thus always lead to a distribution of isolated stars, expanded and already dissolved older clusters and a few deeply embedded still forming embedded clusters with a complex velocity field which also depends on whether the whole cloud was contracting or expanding (Sec. 1.1.2). Observationally, this activity leaves, in association with observational measurement uncertainties, a population of stars which appears non-optimal and even with an age, spin and chemical spread (Kroupa, 1995a,b; Weidner et al., 2009; Marks et al., 2011; Oh and Kroupa, 2012; Oh et al., 2015; Oh and Kroupa, 2016, 2018).

The problem, to which degree an apparent probabilistic quality emerges from an optimally mono (age, metallicity, spin) case may be an interesting research project worthy of study.

Movies based on these publications are available on youtube: "Dynamical ejection of massive stars from a young star cluster" by Seungkyung Oh.

1.5 Does the IMF vary?

Having discussed above the question of whether the IMF is a PDF or an ODF, another problem to deal with is whether the shape of the distribution function varies systematically with the physical conditions of star formation.

As discussed in Sec. 1.3 the consensus has been that the IMF is an invariant PDF, possibly with an upper stellar mass limit near 150 M_{\odot} to 300 M_{\odot} . This was taken to be the case in most studies requiring the stellar populations in star clusters and galaxies. But, as discussed at some length in Kroupa et al. (2013), this consensus may deem unnatural, because different physical conditions should lead to different distributions of stellar masses. The most elementary and thus fundamental and solid arguments, based on the Jeans fragmentation scale (Larson, 1998) on the one hand side, and on self regulation on the other (Adams and Fatuzzo, 1996; Matzner and McKee, 2000; Federrath et al., 2014; Federrath, 2015), lead to the same expectation of how the IMF should change with temperature and metallicity of the gas cloud from which the stars form. Additional physical processes, such as the coagulation of contracting pre-stellar cores in very high-density star-forming regions (Dib et al. 2007, see also Zinnecker and Yorke 2007 and Krumholz 2015 for reviews on the formation of massive stars) and the heating of the molecular gas though an elevated flux of supernova-generated cosmic rays in star-burst regions (Papadopoulos and Thi, 2013), are likely to play a role in establishing a systematic variation of the IMF. All these broad physical arguments lead to the following theoretical expectation:

THE THEORETICALLY EXPECTED VARIATION OF THE IMF:

The IMF should become systematically top-heavy with increasing density, increasing temperature and decreasing metallicity. The empirical boundary condition is that, for the star-formation conditions evident in the present-day Milky Way, the IMF should be close to canonical. This variation may involve α_3 decreasing (the IMF becoming more top-heavy) for decreasing metallicity and increasing density, and for α_1 and α_2 to increase (the IMF becoming bottom-heavy) for increasing metallicity, but a robust prediction as to how the shape of the IMF should vary with conditions does not exist to-date.

Perhaps the first suggestion, based on direct star counts, as to a variation of the IMF with metallicity, has been described in Kroupa (2001, 2002b). Here it was pointed out that, taken at face value, the available resolved stellar populations indicate a systematic flattening of α_1 and of α_2 with decreasing metallicity valid for $[Fe/H] \gtrsim -2$. If such a systematic effect is

present, then for $m < 1 M_{\odot}$ (i = 1, 2) and to first order,

$$\alpha_i \approx 1.3 + \Delta \alpha \log_{10}(Z/Z_{\odot}),$$
(1.8)

with $\Delta \alpha \approx 0.5$ (Kroupa, 2001) (here writing the dependent on metallicity, Z, rather than the iron abundance). The evidence was limited to late-type stars because most of the populations at disposal were old. Concerning massive stars, in a great observational effort, Massey (2003) demonstrated a high degree of invariance of α_3 on density and metallicity for young populations of stars in the Milky Way, the Large and Small Magellanic Clouds. More recently, due to improved data reaching into more extreme star-forming environments, explicit evidence for a systematic variation of α_3 with physical conditions may have begun to emerge on star-cluster scales (Box Observational Constraints II).

Observational Constraints II:

- The high dynamical mass to light ratios of many ultra compact dwarf (UCD) galaxies, which have present-day stellar masses larger than $10^6 \, M_{\odot}$, can be understood if they formed under high density, ρ , with α_3 becoming smaller (more top-heavy) with increasing UCD mass (thus increasing ρ), such that a larger fraction of their initial mass ends up in stellar remnants (Dabringhausen et al., 2009; Jeřábková et al., 2017).
- The high X-ray luminosity of many UCDs can be understood if they have a larger fraction of low-mass X-ray binaries which need a larger fraction of neutron stars and stellar black holes. The data suggest α_3 to become smaller with increasing UCD mass and thus ρ (Dabringhausen et al., 2012).
- The above two points lead to similar constraints on how α_3 varies with ρ . This is an important consistency check. The systematic variation of α_3 with star-formation density implies significant expansion of the UCDs with time due to mass loss from expelled residual gas and from stellar evolution (Dabringhausen et al., 2010). This work demonstrates that the solutions for α_3 also lead to stellar-dynamical solutions to the observed UCDs (they do not dissolve due to too much mass loss).
- Combining the information on an observed systematic deficit of low mass stars in present-day stellar mass functions in observed globular clusters (GCs) with their present-day radii and metallicities, with

stellar-dynamical models which are initially mass segregated and allow for expulsion of residual gas and thus expansion of the young GCs and with the above constraints on $\alpha_3(\rho)$, yields the description of how α_3 depends on ρ and Z given by Eq. 1.9 below from Marks et al. (2012) (see also Kroupa et al. 2013).

- The observed star clusters in M31 are consistent with the dependency formulated as Eq. 1.9 (Zonoozi et al., 2016; Haghi et al., 2017).
- The young ($\approx 1 \,\mathrm{Myr}$), compact (half-mass radius $r_h \approx 1 \,\mathrm{pc}$) $M_{\mathrm{st}} \approx 10^5 \,M_{\odot}$ -heavy star-burst cluster R136 in the 30 Dor star-forming region in the Large Magellanic Cloud has been ejecting its massive stars efficiently. Adding these back statistically into the star-counts in the cluster yields a top-heavy IMF (Banerjee and Kroupa, 2012).
- The stellar census in the massive star-forming region 30 Dor in the Large Magellanic Cloud has been found to have a top-heavy IMF (Schneider et al., 2018), confirming the Banerjee and Kroupa (2012) prediction.
- Deep adaptive optics imaging of the Magellanic Bridge Cluster NGC 796 reveals a top-heavy IMF (Kalari et al., 2018).
- Using multi-epoch Hubble Space Telescope observations of the Arches cluster (2–4 Myr old, $M_{\rm ecl} \approx 4-6\times 10^4\,M_{\odot}$) near the Galactic Centre, Hosek et al. (2019) find the IMF to be top-heavy.

The Empirical IMF Dependence on Density and Metallicity – the initial conditions of stellar populations: Resolved stellar populations largely show an invariant IMF (Eq. 1.1), but for star-formation rate densities $SFRD \gtrsim 0.1\,M_{\odot}/({\rm yr~pc^3})$ in embedded clusters, the IMF appears to become top-heavy (Marks et al., 2012). The dependence of α_3 on cluster-forming cloud density, ρ , (stars plus gas) and Z can be parametrised as

$$\alpha_3 = \alpha_2, \qquad m > 1 M_{\odot} \qquad x' < -0.87,
\alpha_3 = -0.41 \times x' + 1.94, \quad m > 1 M_{\odot} \qquad x' \ge -0.87,$$
(1.9)

$$x' = -0.14 \log_{10}(Z/Z_{\odot}) + 0.99 \log_{10}\left(\rho/\left(10^6 M_{\odot} \,\mathrm{pc}^{-3}\right)\right). \tag{1.10}$$

A possible variation of the IMF for late-type stars with Z is suggested by Eq. 1.8. In Eq. 1.9, the density (stars plus gas at a mathematical time, t_{math} , when all the stars have been born and the remaining gas

has not yet been expelled) of the star-forming molecular cloud clump is

$$\rho = \frac{3 \ (M_{\rm ecl}/2)}{4 \pi \epsilon \, r_h^3},\tag{1.11}$$

where the star-formation efficiency, ϵ , is Eq. 1.4 and r_h is Eq. 1.5 being the half-mass radius of the clump. Note that this clump, or rather embedded cluster, is a mathematical hilfskonstrukt which in reality does not exist because the alluded to mathematical time does not exist. In reality the stars of the embedded cluster form over about 1 Myr and the gas is blown out over a time which may be approximated by the sound speed of ionised gas ($\gtrsim 10 \, \mathrm{km/s}$, e.g. the extremely young Treasure Chest cluster, Smith et al. 2005, and the massive star-burst clusters in the Antennae galaxies, Whitmore et al. 1999; Zhang et al. 2001) and r_h . The stars form in filaments rather than spherical Plummer models. Nevertheless, by dynamical equivalence, any two dynamical structures (e.g. the Plummer model and a filament) lead to comparable dynamical processing of the stars formed within them if the two structures are dynamically equivalent (Kroupa, 1995a; Belloni et al., 2018). By conservation of angular momentum, stars need to form in multiple systems, whereby most form as binaries (Goodwin and Kroupa, 2005) with well defined orbital parameter distributions and internal (eigen) evolutionary processes (Kroupa, 1995b; Belloni et al., 2017). But at the extreme density needed for the top-heavy IMF regime, our knowledge of the processes within the forming cluster remain poor. Formally, in this regime, the crossing time is shorter than the formation time of a single proto star ($\approx 10^5 \, \mathrm{yr}$).

In conclusion, high-quality star-count data appear to suggest a systematic variation of the IMF. Eq 1.9 and 1.8 are possible quantifications of this variation with density and metallicity of the star-forming gas cloud. The above observational findings are compared in Fig. 1.4. This variation is consistent with the qualitative expectations from star-formation theory noted at the beginning of this section. Extending the analysis to unresolved young clusters in other galaxies will prove to be an important consistency test whether this formulation of the variation is a good approximation (e.g. Ashworth et al. 2017).

If true, this IMF variation has important implications for galaxy-wide IMFs, and also impinges on the interpretation of the IMF as a PDF. If the IMF varies as suggested here and if it is to be a PDF, then it can only be a constrained PDF, because, before beginning the stochastic drawing

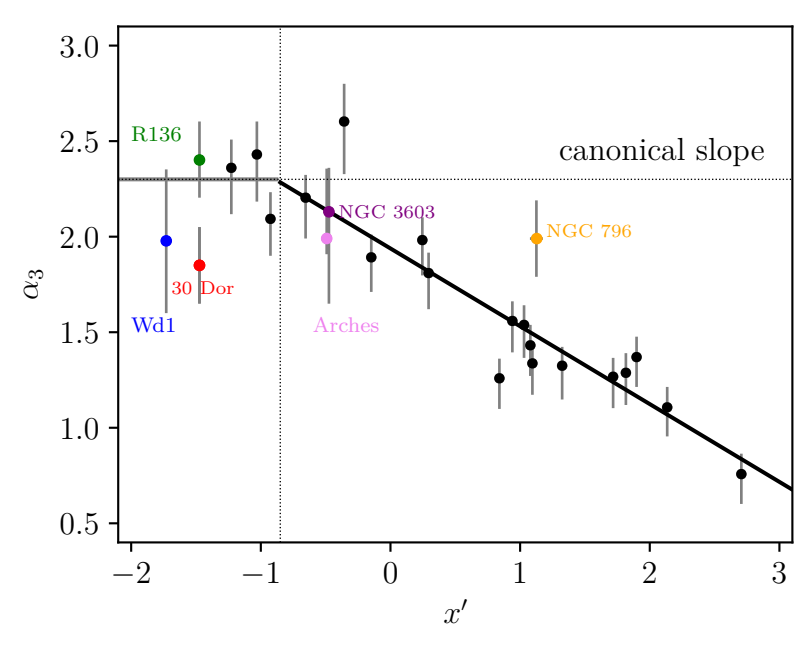


Figure 1.4 The variation of the upper end of the stellar IMF with metallicity and cloud density (solid line, Eq. 1.9) as deduced from deep observations of MW GCs using a principal-component-type analysis (Marks et al., 2012). The recent observational determination of top-heavy IMFs in two metalpoor very young clusters (30Dor: Schneider et al. 2018, NGC796: Kalari et al. 2018) and the recent Arches data (Hosek et al., 2019) are included with the data shown here. Adapted from Marks et al. (2012).

process, the functional form of the IMF needs to be calculated based on the properties of the embedded cluster, which however itself is supposedly drawn stochastically from an embedded cluster mass function. It remains to be seen, perhaps more from a philosophical point of view, if and how a PDF interpretation of the IMF is satisfyingly compatible with a systematic variation of the IMF given by the physical conditions at star formation, since one would, on the one hand side, be resorting to a stochastic process, but on the other hand side, also to to a process driven by physical conditions.

1.6 Is the IMF of a simple stellar population equal to that of a composite population?

Consider a single star-forming region and a region containing many starforming regions, such as a whole galaxy. We can then define the IMF of the larger region to be the composite IMF, cIMF. Considering a whole galaxy, the cIMF becomes equal to the galaxy-wide IMF (gwIMF, Kroupa and Weidner 2003).

THE COMPOSITE IMF STATEMENT:

Logically, the cIMF is the sum of all IMFs assembled throughout the region within some time δt .

From Eq. 1.2 and 1.3: for any pair m_1, m_2, X_{12} (calculated assuming $\xi_{\rm p}(m)$ is the PDF corresponding to the IMF) will be equal to another X_{12} (calculated assuming $\xi_{\rm p}(m)$ is the PDF corresponding to the cIMF) if and only if both PDFs are equal because m_1 and m_2 are arbitrary. This is the fundamental composite IMF-PDF theorem (see also Kroupa and Jerabkova 2018):

THE COMPOSITE IMF-PDF THEOREM:

If the IMF is a PDF then the IMF of all stars formed in a galaxy within a short time interval δt , the galaxy-wide IMF (gwIMF), is equal to the IMF.

This theorem has been applied in most studies of star-formation in galaxies. In particular, the Kennicutt SFR–H α tracer rests on assuming this theorem holds (Kennicutt, 1998; Jeřábková et al., 2018). It assumes that any sum of IMFs will yield the same PDF which is true if all individual IMFs are fully sampled over all possible stellar masses. But is this formulation applicable to real galaxies?

Solving this problem is of paramount importance for measuring SFRs. If the IMF is invariant and equal to the gwIMF then the tracer can be calibrated simply and becomes invariant to galaxy type and mass. For example, the number of recombination photons per unit time, i. e. the H α flux, which is proportional to the number per unit time of ionising photons emitted by a fresh stellar population, depends on the number of the ionising (i.e. massive, $m \gtrsim 10 \, M_{\odot}$) stars in the young population. If the gwIMF is invariant and equal to the IMF and both are fully sampled up to $m_{\rm max*}$, then the H α flux is a direct measure of the total mass of stars born per unit time (Kennicutt, 1998). For this calibration to remain valid, the IMF needs to be an invariant PDF. In star-by-star models of galaxies this interpretation is equivalent to a stochastic description of star formation without constraints.

1.6.1 Clustered star formation, but star formation is stochastic

If stars form in embedded clusters (e.g. Hopkins 2013b) which are randomly distributed throughout a galaxy and which follow a distribution of masses, i.e. an ECMF (Eq. 1.13 below), then two possibilities arise:

1. The cluster mass in stars, $M_{\rm ecl}$, plays no role and stars appear randomly filling a cluster to a pre-specified maximum number of stars, $N_{\rm ecl}$. This yields a distribution of clusters with different numbers of stars, and thus to an ECMF. Within each cluster the IMF is sampled randomly without constraints, apart from the condition that stars have masses $m \leq m_{\text{max}}$. In this case the composite IMF-PDF theorem (p. 28) holds, making gwIMF equal in form to the IMF and any tracer of star formation rate (e.g. the Kennicutt SFR-H α tracer, Kennicutt 1998) will yield a correct value of the SFR upon measurement of the tracer (e.g. the H α flux) subject to stochastic variations. This interpretation implies that a "cluster" may consist of one massive star only. Thus, isolated massive stars would pose an important argument for this purely stochastic approach to galaxy evolution. This possibility implies that a $m_{\text{max}} - N_{\text{ecl}}$ relation does not exist. A $m_{\rm max}-M_{\rm ecl}$ relation emerges but has a large scatter consistent with random drawing from the IMF (Maschberger and Clarke, 2008). An issue with this possibility is that the primary variable, $N_{\rm ecl}$, needs to be interpreted as a physical parameter.

If nature were to follow this mathematical recipe, then the measured SFRs, using the Kennicutt SFR-H α tracer for example, will appropriately assess the true SFRs. Galaxies with very small SFRs will show a dispersion of SFRs which increases with decreasing SFR as a result of stochasticity.

2. Considering $M_{\rm ecl}$ to be the primary variable, and choosing it randomly from the ECMF, the embedded cluster is filled with stars randomly from the IMF until the mass of the stellar population matches $M_{\rm ecl}$. This is constrained random sampling (Weidner and Kroupa, 2006; Weidner et al., 2010, 2013c). If the ECMF contains clusters with $M_{\rm ecl} < m_{\rm max*}$ then in these clusters, the stellar population will lack the most massive stars. Such clusters are undersampling the IMF at large stellar masses. The deficit arises because a cluster of mass $M_{\rm ecl} < m_{\rm max*}$ cannot contain a star weighing more than the cluster. The whole population of all embedded clusters will thus have a systematic deficit of the most massive stars, i.e. the gwIMF will be under-sampled at high stellar masses and will not equal the IMF. This possibility implies a $m_{\rm max} - M_{\rm ecl}$ relation which has a large scatter, since there may exist a cluster of mass $M_{\rm ecl}$ being composed off one star of mass $m = M_{\rm ecl}$. The existence of isolated massive stars is if paramount importance for this possibility to be valid.

This implies that any tracer of ionising stars, calibrated assuming the first possibility above, will systematically underestimate the true SFR of the region or galaxy in cases when under-sampled clusters are involved.

This case has been extensively studied in the SLUG approach (da Silva et al., 2012, 2014).

If nature were to follow this mathematical recipe, then the measured SFRs, using the Kennicutt SFR-H α tracer for example, will deviate systematically towards smaller-than- $SFR_{\rm true}$ -values at low SFRs. Galaxies with very small SFRs will show a dispersion of SFRs which increases with decreasing SFR as a result of stochasticity (fig. 3 in da Silva et al. 2014).

1.6.2 Clustered star formation, but star formation is optimal

The above two stochastic approaches are consistent with the notion that galaxies have a stochastic history which comes about from the need of a very large number of mergers to build-up Milky-Way-class disk galaxies in the standard LCDM cosmological model. The observed simplicity of galaxies (Disney et al., 2008) and lack of evidence for an intrinsic dispersion in the baryonic-Tully-Fischer relation (McGaugh, 2005, 2012), in the mass-discrepancy relation (McGaugh, 2004) and in the radial-acceleration relation (McGaugh et al., 2016; Lelli et al., 2017) as well as the existence of a tight and well defined main sequence of galaxies over different red-shifts (Speagle et al. 2014), indicate that the dynamical structure and the star-formation behaviour of galaxies may follow precise rules and that the expected stochasticity may be absent (Disney et al., 2008).

Observations have shown that stars form in molecular clouds (Sec. 1.1.2). This suggests that if the IMF were to be a PDF, then this PDF should be subject to constraints: stars do not form at arbitrary positions within a galaxy, they do so only where the conditions allow their formation. Since the conditions and properties of molecular clouds change with position in a galaxy (notably, inner region versus the far outer region, Fukui and Kawamura 2010; Heyer and Dame 2015) the possibility might be given that the constraints subjecting the PDF also depend on position within the galaxy and within molecular clouds (see Box Observational Constraints III on p. 30).

BOX OBSERVATIONAL CONSTRAINTS III:

• Stars do not form randomly throughout molecular clouds but in embedded clusters (Sec. 1.1.2). The observed distributed population is explainable through the dynamical activity of the forming embedded clusters (Sec. 1.4.3).

- The mixture of embedded clusters determines the cIMF of a region in the molecular cloud (Hsu et al., 2012). According to the discussion in Sec. 1.4.1, stars form in filaments which combine to embedded clusters which are mass-segregated (Box Observational Constraints I on p. 16).
- The distribution of young star-cluster masses shows a radial gradient with the most-massive cluster within a radial annulus being smaller at larger galactocentric distance in the disk galaxy M33 for example (Pflamm-Altenburg et al., 2013). This is a result of the exponentially declining surface mass-density of gas in a disk galaxy.
- A decreasing cluster-mass with galactocentric-distance relation is also found in the interacting interacting LIRG Arp 299 system as a result of the gas density distribution (Randriamanakoto et al., 2018).
- The formation of the embedded most massive stellar sources shows a Galactocentric radially decreasing trend in the Milky Way (Urquhart et al., 2014) reminiscent of the above M33 result.
- Late-type galaxies show a pronounced correlation between their SFR and their most massive very young cluster, the $M_{\rm ecl,max} SFR$ relation (Weidner et al., 2004). The dispersion of the data is consistent with observational uncertainty, and Randriamanakoto et al. (2013) point out that their own data imply that the dispersion is not consistent with stochastic scatter by being too small.

Is there thus an alternative to the above two stochastic approaches (Sec. 1.6.1) for describing stellar populations in galaxies? Is it possible to derive a theory which has no intrinsic scatter, taking the observed simplicity of galaxies as a motivation? Even in such a theory, an observable dispersion would arise naturally (Sec. 1.4.3), and some intrinsic dispersion can always be added if needed. It might be educational to develop a theory which has no intrinsic scatter to test how applicable this perhaps extreme description may be.

If successful, we will have uncovered the laws of nature which describe how the interstellar medium in a galaxy transforms into a new stellar population and at which rate it does so.

One possibility is to begin with the rules (we may also refer to them as axioms, cf. Recchi and Kroupa 2015; Yan et al. 2017) deduced from observations of star formation within nearby molecular clouds and from very young stellar populations in embedded and older star clusters (e.g. Eqs 1.8 and 1.9, Observational Constrains I–III), assume these rules are valid independently

of cosmological epoch and calculate how they imply what galaxies with different properties ought to look like in their star formation behaviour. This approach has the advantage that it (by construction) fulfils all observational constraints (as outlined in Observational Constraints I–III), and that it is, in particular, consistent with the stellar mass functions in the observed star clusters and the Galaxy. These observations suggest that star formation may be significantly regulated, possibly following precise and clear rules.

In addition to the two above stochastic approaches (Sec. 1.6.1), we may therefore entertain a model in which star-formation is entirely optimal on every scale.

Once we know how to compute such a model, it is clear that it becomes completely predictive. Some scatter in observable properties then enters via physical processes (e.g. galaxy–galaxy encounters which change the mass distribution and SFR over some time), other physical processes (Sec. 1.4.3) and measurement errors. The question is now how to construct such a deterministic, optimal, model?

We thus begin with "The composite IMF statement" (p. 28): If each embedded cluster⁴ spawns a population of stars (this takes $\lesssim 1 \,\mathrm{Myr}$) with combined mass $M_{\rm ecl}$ per cluster, then the gwIMF becomes an integral over all such embedded clusters within the galaxy, yielding the integrated galaxywide initial mass function (IGIMF, Eq. 1.12; Kroupa and Weidner 2003; Weidner and Kroupa 2005; Yan et al. 2017; Jeřábková et al. 2018). A clue that this may be an interesting avenue to investigate is provided by the galactic-field gwIMF being steeper than the canonical IMF for $m>1\,M_{\odot}$ (Scalo 1986; Kroupa et al. 1993; Rybizki and Just 2015; Mor et al. 2017, 2018; Sec. 1.3): this difference might be related to the gwIMF being a sum of the IMFs in the star-forming units (Kroupa and Weidner, 2003; Zonoozi et al., 2019). The IGIMF is a particular mathematical formulation of the gwIMF. The embedded clusters need to be sampled (e.g. optimally, Schulz et al. 2015) from the ECMF. This means that over some time interval, δt , the ECMF is optimally assembled, whereby this time interval needs to be investigated with care⁵.

⁴ An embedded cluster can be constructed to be optimal by it being mass segregated initially and by it following the $m_{\rm max}-M_{\rm ecl}$ relation (Pavlík et al., 2019). Initially mass segregated models in dynamical equilibrium, such that the mass segregation would persist in collision-less systems, can be constructed using the methods developed in Bonn, namely by energy-stratifying the binary systems in the clusters (Šubr et al., 2008; Baumgardt et al., 2008). The embedded clusters can be optimally distributed throughout the galaxy by associating the most massive cluster at any galactocentric radius with the local gas surface density (Pflamm-Altenburg and Kroupa, 2008).

⁵ Note that here the optimal model is being formulated. It is possible to relax the inherent non-dispersion nature and to retain the IGIMF formulation (Eq. 1.12) but to treat the

DEFINITION: The IGIMF is an integral over all star-formation events (embedded clusters, Sec. 1.1.2) in a given star-formation "epoch" $t, t + \delta t$,

$$\xi_{\text{IGIMF}}(m;t) = \int_{M_{\text{ecl,min}}}^{M_{\text{ecl,max}}(SFR(t))} \xi\left(m \le m_{\text{max}}\left(M_{\text{ecl}}\right)\right) \ \xi_{\text{ecl}}(M_{\text{ecl}}) \ dM_{\text{ecl}},$$
(1.12)

with the normalisation conditions Eqs. 1.15 and 1.16 below and also with the conditions Eqs. 1.6 and 1.7 which together yield the $m_{\rm max}-M_{\rm ecl}$ relation

Here $\xi(m \leq m_{\rm max})$ $\xi_{\rm ecl}(M_{\rm ecl})$ $dM_{\rm ecl}$ is the composite stellar IMF (i.e. the cIMF) contributed by $\xi_{\rm ecl}$ $dM_{\rm ecl}$ embedded clusters with stellar mass in the interval $M_{\rm ecl}$, $M_{\rm ecl} + dM_{\rm ecl}$. The ECMF is often taken to be a power-law,

$$\xi_{\rm ecl}(M_{\rm ecl}) \propto M_{\rm ecl}^{-\beta},$$
 (1.13)

with $\beta \approx 2$ (Lada and Lada 2003; Schulz et al. 2015 and references herein). For the Milky Way and extra-galactic data on non-star-bursting galaxies, $\beta \approx 2.3$ may be favoured (Weidner et al., 2004; Mor et al., 2018), and β may vary with the metallicity and SFR (Yan et al., 2017).

The most-massive embedded cluster forming in a galaxy, $M_{\rm ecl,max}(SFR)$, can be assumed to come from the empirical maximum star-cluster-mass vs global-star-formation-rate-of-the-galaxy relation,

$$M_{\rm ecl,max} = 8.5 \times 10^4 \left(\frac{\rm SFR}{M_{\odot}/\rm yr} \right)^{0.75},$$
 (1.14)

(eq. 1 in Weidner and Kroupa 2005, as derived by Weidner et al. 2004 using observed maximum star cluster masses). A relation between $M_{\rm ecl,max}$ and SFR, which is a good description of the empirical data, can also be arrived at by resorting to optimal sampling (Sec. 1.4.2). Thus, when a galaxy has, at a time t, a SFR(t) which is approximately constant over a time span δt over which an optimally sampled embedded star cluster distribution builds up with total mass $M_{\rm tot}(t)$, then there is one most massive embedded cluster with mass $M_{\rm ecl,max}$,

$$1 = \int_{M_{\text{ecl,max}}(t)}^{M_{\text{U}}} \xi_{\text{ecl}}(M_{\text{ecl}}) dM_{\text{ecl}}, \qquad (1.15)$$

with $M_{\rm U}$ being the physical maximum star cluster than can form (for prac-

sampling of embedded star cluster masses and of stars within the embedded clusters stochastically. This was the original notion followed by Kroupa and Weidner (2003) and forms the basis of the SLUG approach (da Silva et al., 2014).

34 The initial mass function of stars and the star-formation rates of galaxies tical purposes $M_{\rm U} > 10^8 \, M_{\odot}$), and

$$SFR(t) = \frac{M_{\text{tot}}(t)}{\delta t} = \frac{1}{\delta t} \int_{M_{\text{ecl,min}}}^{M_{\text{ecl,max}}(t)} M_{\text{ecl}} \, \xi_{\text{ecl}}(M_{\text{ecl}}) \, dM_{\text{ecl}}. \tag{1.16}$$

 $M_{\rm ecl,min}=5\,M_{\odot}$ is adopted in the standard modelling and corresponds to the smallest "star-cluster" units observed (the few M_{\odot} -heavy embedded clusters in fig. 1 in Yan et al. 2017 such as are observed in Taurus-Auriga, e.g. Kroupa and Bouvier 2003; Joncour et al. 2018). Note the similarity of these equations with Eqs. 1.6 and 1.7. Perhaps the physical meaning of this is that within a galaxy the formation of embedded clusters may be a self-regulated growth process from the ISM, like stars in a molecular cloud core which spawns an embedded cluster.

But what is δt ? Weidner et al. (2004) define δt to be a "star-formation epoch", within which the ECMF is sampled optimally, given a SFR. This formulation leads naturally to the observed $M_{\rm ecl,max}(SFR)$ correlation if the ECMF is invariant, $\beta \approx 2.35$ and if the "epoch" lasts about $\delta t = 10$ Myr. Under these conditions, a galaxy forms embedded clusters with stellar masses ranging from $M_{\rm ecl,min} = 5 \, M_{\odot}$ to $M_{\rm ecl,max}$, the value of which increases with the SFR of the galaxy in accordance with the observed young most-massive cluster vs SFR data (Box Observational Constraint III on p. 30). Thus, the embedded cluster mass function is optimally sampled in about 10 Myr intervals, independently of the SFR.

It is interesting to note now that this time-scale is consistent with the star-formation time-scale in normal galactic disks measured by Egusa et al. (2004, 2009, 2017) using the offset of HII regions from the molecular clouds in spiral-wave patterns. In this view, the ISM takes about 10 Myr to transform via molecular cloud formation to a new population of young stars which optimally sample the embedded-cluster mass function (see also Sec. 1.1.2). Schulz et al. (2015) discuss (in their Sec. 3) the meaning and various observational indications for the time-scale $\delta t \approx 10\,\mathrm{Myr}$. This agreement between the independent methods to yield $\delta t \approx 10\,\mathrm{Myr}$ is encouraging, since the Weidner et al. (2004) argument is independent of the arguments based on molecular cloud life times and spiral arm phase-velocities.

The IGIMF (Eq. 1.12) can be calculated under various assumptions on how the IMF, $\xi(m)$, varies with physical conditions. Ignoring the explicit metallicity dependence but taking into account the effective density dependence, which includes an intrinsic metallicity dependence, in Eq. 1.9 above, Yan et al. (2017) studies the prediction of the IGIMF theory for the variation of the shape of the gwIMF in comparison with observational constraints (Fig. 1.6). The change of the IGIMF as a function of the SFR is shown in

Fig. 1.5. The observational constraints, which indicate the gwIMF to change from a top-light form (i.e. with a deficit of massive stars) in dwarf galaxies (which have low SFRs, Lee et al. 2009) to top-heavy gwIMFs in massive late-type galaxies (which have high SFRs, Gunawardhana et al. 2011), are well covered by the IGIMF theory. It is noted here for completeness that the top-light gwIMF variation for dwarf galaxies was predicted on the basis of the IGIMF theory (Pflamm-Altenburg et al., 2007, 2009) before the data were available, with observational support from star-counts being found by Watts et al. (2018) in DDO154. The calculations of the IGIMF for galaxies with high SFRs became physically relevant once the variation of the IMF (Eq. 1.8 and 1.9) in extreme star-burst clusters became quantified based on observational data (Marks et al., 2012).

A full-gird of IGIMF models is provided by Jeřábková et al. (2018) in which three cases are considered: (1) The IMF is invariant, (2), the IMF varies only at the massive end (Eq. 1.9), and (3) the IMF varies at low (Eq. 1.8) and at high (Eq. 1.9) masses. This latter case, IGIMF3, is considered to be the most realistic, and appears to be able to account for the complicated time-evolving gwIMF variation deduced to have occurred when elliptical galaxies formed, as well as for the gwIMF variations deduced for late-type galaxies.

1.6.3 Some observational constraints

Any of the three approaches, namely pure stochastic sampling (Sec. 1.6.1), constrained stochastic sampling (Sec. 1.6.1) and the IGIMF formulation in terms of optimal systems (Sec. 1.6.2), need to be consistent with observational constraints. Some relevant ones can be found in Box Observational Constraints IV (p. 35).

BOX OBSERVATIONAL CONSTRAINTS IV:

- Dwarf late-type galaxies, with typically small ($\approx 0.0001 0.1 \, M_{\odot}/\mathrm{yr}$) to extremely small ($\lesssim 10^{-4} \, M_{\odot}/\mathrm{yr}$) SFRs, have been found to have a systematically increasing deficit of H α emission relative to their UV emission with decreasing SFR. This can be readily understood as a result of an increasingly top-light gwIMF (Lee et al., 2009).
- Direct (star-count) evidence supporting this comes from the nearby dwarf galaxy DDO154 (Watts et al., 2018) and from Leo P (Jeřábková

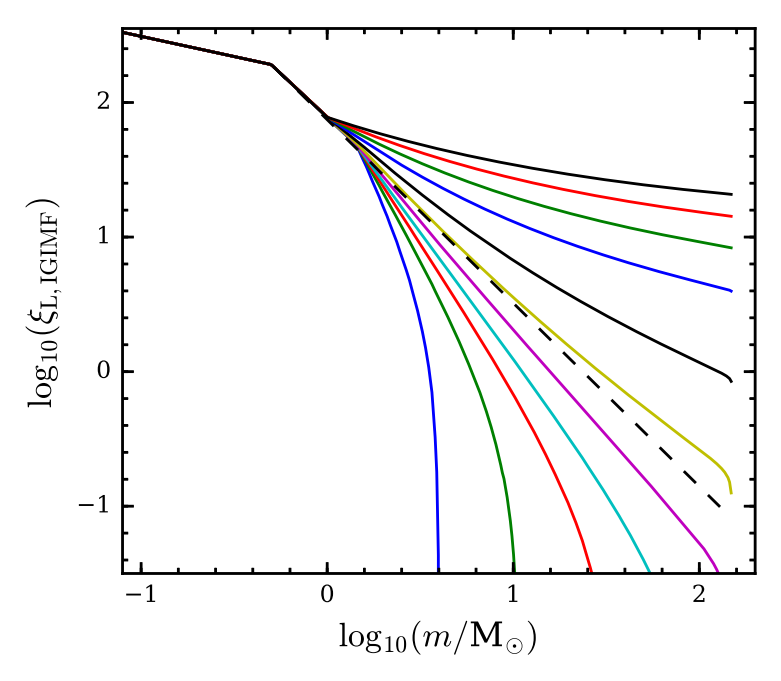


Figure 1.5 Logarithmic integrated gwIMFs (in number of stars per logmass interval, using the transformation $\xi_{\rm L}=m\ln(10)\,\xi(m)$, eq. 14 in Yan et al. 2017), for different SFRs and formed over a $\delta t=10\,{\rm Myr}$ epoch. Each line is normalised to the same values at $m<1\,M_\odot$. Solid curves are IGIMFs for $SFR=10^{-5},10^{-4}...10^5\,M_\odot/{\rm yr}$ from bottom left to top right. The dashed line is the canonical IMF (Eq. 1.1). For further details see Yan et al. (2017). Note that the explicit metal dependency of the IGIMF is not included in these calculations and that the $\alpha_3^{\rm gal}$ values plotted in Fig. 1.6 are the slopes of the here shown IGIMFs in different stellar mass ranges. See Jeřábková et al. (2018) for a full grid of IGIMF models in dependency of metallicity and SFR.

et al., 2018). Both galaxies have a deficit of massive stars, i.e. appear to have a top-light gwIMF.

- The chemical properties of the low-mass satellite galaxies of the Milky Way, for which sufficient data exist, suggest they had gwIMFs with a deficit of massive stars (Tsujimoto, 2011). This is consistent with the above two points.
- Massive late-type galaxies, with typically large ($\gtrsim 1\,M_\odot/\mathrm{yr}$) SFRs, have been found to have a systematically more top-heavy gwIMF with increasing SFR, as deduced from their H α flux and broad-band optical colours. This can be understood as a result of an increasingly

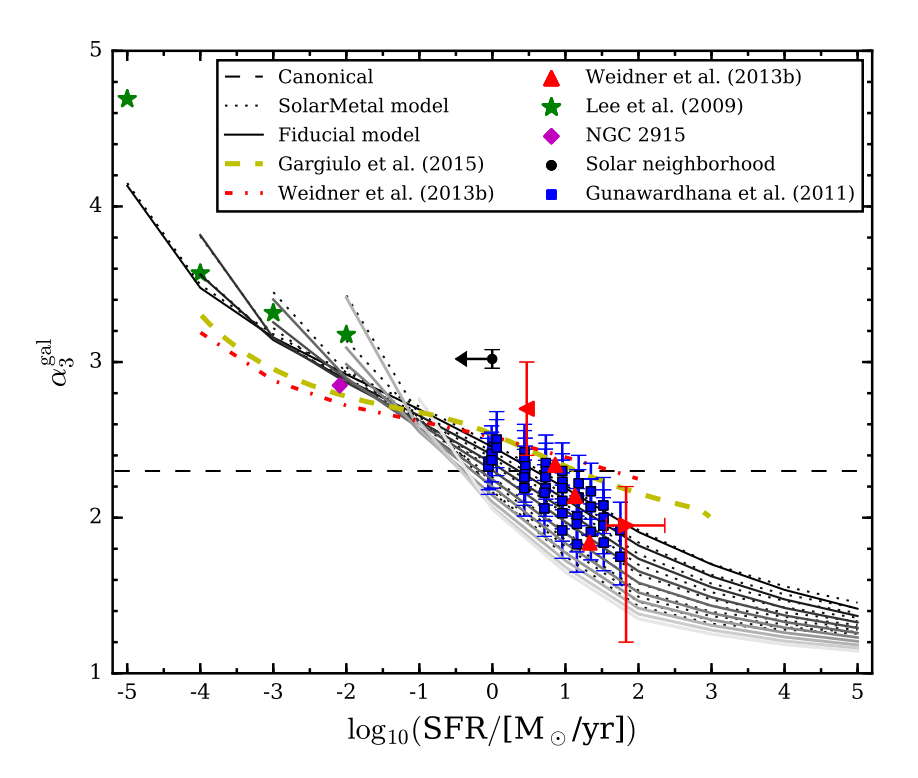


Figure 1.6 The variation of the IGIMF power-law index $\alpha_3^{\rm gal}$ (for stars with $m>1\,M_{\odot}$) with the galaxy-wide SFR is shown as the lines. Each line is an evaluation of the index at a particular stellar mass, showing that the IGIMF is curved since $\alpha_3^{\rm gal}$ changes with m (Fig. 1.5). The invariant canonical IMF is shown as the horizontal dashed line, values above it are top-light gwIMFs and below it are top-heavy gwIMFs. The solid and dotted lines constitute, respectively, the fiducial model (which includes an effective metallicity dependence in the density dependence of the IMF) and the Solar-abundance model (for details see Yan et al. 2017). The dot-dashed and dashed coloured lines are IGIMF models from Gargiulo et al. (2015) and Weidner et al. (2013b). The symbols are various observational constraints as indicated in the key. From Yan et al. (2017).

top-heavy gwIMF (Gunawardhana et al., 2011). Evidence for this has been found before also (Hoversten and Glazebrook, 2008; Meurer et al., 2009).

• Massive elliptical galaxies have been found to have formed rapidly (within a Gyr) with $SFR \gtrsim 10^3 \, M_{\odot}/{\rm yr}$, as deduced from their high alpha-element abundances (Thomas et al., 2005; Recchi et al., 2009). Their high metallicity required them to have had top-heavy gwIMFs

- to generate the large mass in metals within the short time (Matteucci, 1994; Vazdekis et al., 1997; Weidner et al., 2013b,a; Ferreras et al., 2015; Martín-Navarro, 2016). This fits well into the above three points which suggest a general shift of the gwIMF towards producing more massive stars relative to the low-mass stellar content with increasing SFR.
- The isotopes, 13 C and 18 O, are, respectively, released mainly by lowand intermediate-mass stars ($m < 8\,M_{\odot}$) and massive stars ($m > 8\,M_{\odot}$). Using the ALMA facility, Zhang et al. (2018) measured rotational transitions of the 13 CO and 18 O isotopologues in a number of star-bursting galaxies ($SFR \gtrsim 10^3\,M_{\odot}/\mathrm{yr}$) finding strong evidence for the galaxy-wide IMF to be top-heavy.
- Massive elliptical galaxies also show evidence that they had a significantly bottom-heavy IMF (van Dokkum and Conroy 2010; Conroy and van Dokkum 2012; Martín-Navarro 2016 and references therein).
- Early-type galaxies have a trend in metallicity and alpha-element abundances explainable with an increasingly top-light gwIMF with decreasing galaxy mass and thus decreasing SFR during their formation (Köppen et al., 2007; Recchi et al., 2009; Recchi and Kroupa, 2015). Alternatively, element-selective outflows from star-forming galaxies may account for the observed mass-metallicity relation among galaxies. Observational surveys to establish this have failed to detect evidence for outflows (Lelli et al., 2014; Concas et al., 2017), although McQuinn et al. (2018) report observation of hot gas leaving star-bursting dwarf galaxies.
- Disk galaxies have an H α cutoff radius beyond which H α emission is significantly reduced or absent compared to the UV emission (Boissier et al., 2007). These UV-extended disks can be understood in terms of a galactocentric-radial dependency of the ECMF (see Box Observational Constraints III on p. 30) in combination with the $m_{\rm max}-M_{\rm ecl}$ relation (Fig. 1.3) such that the typically low-mass embedded clusters forming in the outer regions come along with a stellar population which is deficient in ionising radiation (Pflamm-Altenburg and Kroupa, 2008).

Is it possible that instead of the optimal star formation theory developed above (Sec. 1.6.2), the gwIMF remains universal and invariant and that star formation is stochastic, perhaps in a constrained manner such as in the SLUG approach (Sec. 1.6.1), and that the observed correlations in and among galaxies (Box Observational Constraints IV on p. 35) are due to

photon leakage, dust obscuration and redenning and other physical effects (Calzetti, 2008, 2013)? It is likely that these are relevant, but the authors of the original research papers reporting the mentioned effects (Hoversten and Glazebrook, 2008; Meurer et al., 2009; Lee et al., 2009; Gunawardhana et al., 2011) discuss these biases at great length disfavouring them. It is nevertheless probably useful to study how invariant but stochastic models might be able to lead to the observed correlations. For example, a systematic deficit of massive stars in dwarf galaxies could come about if the dwarf galaxies are, as a population, going through a current lull in star-formation activity (Kennicutt and Evans, 2012). But this appears contrived and extremely unlikely (Lee et al., 2009), especially since one would need to resort to an in-step height in the SFR of nearby massive disk galaxies in order to explain the general observed shift of a large $H\alpha$ -deficiency becoming smaller through to an $H\alpha$ -emission overabundance when increasing the stellar mass from dwarf to major disk galaxies (Fig. 1.6).

The predictability of the IGIMF theory is an advantage though. It allows testing of the models against data (but the calculations need to be done correctly before drawing conclusions, see the end of Sec. 1.4.1). Also, if found to be a good representation of the observational data, we can use it to learn about star-formation at high redshift and use galaxy-wide star-formation behaviour to constrain star-formation physics on the scales of embedded clusters (Jeřábková et al., 2018).

1.7 Implications for the SFRs of galaxies

Most measures of the SFR of galaxies rely on the photon output from massive stars ($m \gtrsim 10 \, M_{\odot}$) which are the most luminous objects. These are a good probe of the current SFR due to their short life-times ($\lesssim 50 \, \text{Myr}$ before exploding as a core-collapse supernovae, SNII events). For an empirical comparison of the various SFR tracers the reader is referred to Mahajan et al. (2019).

For the purpose of this discussion of how different treatments of the gwIMF may affect SFR measurements we assume the observer detects all relevant photons (i.e. that dust obscuration, photon leakage and other effects – see Calzetti 2008, 2013 for a discussion – have been corrected for) and we concentrate on the H α -based SFR measure (Kennicutt, 1989; Pflamm-Altenburg et al., 2009). It assumes that a fraction of ionising photons ionises hydrogen atoms in the nearby ISM and that these recombine. A fraction of the recombination photons is emitted as H α photons and it has been shown that the flux of these is proportional to the ionising flux such that the H α

luminosity becomes a direct measure of the current population of massive stars. Given their short life-times ($\lesssim 50 \,\mathrm{Myr}$), we thus obtain an estimate of the SFR if we know which mass in all young stars is associated with these ionising stars, i.e if we know the shape of the gwIMF. The H α luminosity is the most sensitive measure of the population of ionising stars (unless direct star-counts can be performed in nearby dwarf galaxies, e.g. Watts et al. 2018). For completeness, we note that the GALEX far-UV (FUV) flux is a measure of the stellar population which includes late-B stars and thus summarises the SFR activity over the recent 400 Myr time window (see Pflamm-Altenburg et al. 2009 who used the PEGASE code, and chapter 7 in the present book for a detailed discussion of the timescales of each SFR indicator but assuming an invariant gwIMF). We do not address this measure here except to note that in the limit where only a few ionising stars form, the FUV-flux derived SFRs are more robust and these are indeed consistent with the higher SFRs as calculated using the IGIMF1 formulation (Jeřábková et al., 2018) as shown explicitly in fig. 8 of Lee et al. (2009), who compare FUV and H α -based SFR indicators for dwarf galaxies. The FUV flux is thus a more robust measure of SFR_{true} than the H α flux because it assesses a much more populous stellar ensemble therewith being less susceptible to Poisson noise, but it is more sensitive to the gwIMF of intermediate-mass stars and also only offers a poorer time resolution (maximally 400 vs maximally 50 Myr, respectively, Pflamm-Altenburg et al. 2009). The rate of SNII also provides a measure, but we do not know which fraction of massive stars implode into a black hole without producing an explosion and how this depends on metallicity and thus redshift. SNII events are too rare on a human life-time to provide reliable global measurements except in profusely star-bursting systems (e.g. as in Arp 220, Dabringhausen et al. 2012 and references therein, Jeřábková et al. 2017).

We refer to $SFR_{\text{H}\alpha}$ as being the SFR measure using the H α flux, and with SFR_{K} we mean $SFR_{\text{H}\alpha}$ in the specific case of using the Kennicutt (1998) calibration which assumes a fully sampled and invariant standard IMF (the Kennicutt IMF, which is very similar to the canonical IMF, Pflamm-Altenburg et al. 2009). Therefore, if the gwIMF differs from the invariant canonical one, then $SFR_{\text{K}} \neq SFR_{\text{true}}$. If the gwIMF were to be invariant and a PDF then the average of SFR_{K} over a sufficiently large number of galaxies of similar baryonic mass (Speagle et al., 2014) would provide the correct measure of the SFR with increasing dispersion with decreasing SFR_{true} (Sec. 1.4.1), $SFR_{\text{true}} = \overline{SFR}_{\text{K}}$. We also consider SFR_{SLUG} which is the H α -based SFR computed within the SLUG approach (Sec. 1.6.1, footnote 2 on p. 21, footnote 5 on p. 32). If reality were to correspond to the assumptions underlying

the SLUG approach (see text below) then $SFR_{SLUG} = SFR_{true}$, since in any particular model galaxy, the SLUG methodology knows what the model gwIMF is, such that the SFR is calculated properly. However, the SLUG approach does not allow to infer the true SFR, SFR_{true} , for an observed galaxy, since, by the stochastic aspect inherent to SLUG, the observer does not know the actual momentary gwIMF. This comes about because for a SFR_{true} in the observed galaxy, the observer does not know whether the gwIMF is more or less top-heavy for example (due to stochastic fluctuations) as long as this gwIMF is consistent with the SFR-tracer (for example, the same $H\alpha$ flux can be obtained by differently shaped gwIMFs). The SFR measure, SFR_{IGIMF} , is likewise based on the H α flux but is calculated taking into account the number of ionising stars in the IGIMF theory (Sec. 1.4.2) such that $SFR_{IGIMF} = SFR_{true}$ without scatter (apart from variations at the very small SFR_{true} level where a single ionising star may be born or die, see Pflamm-Altenburg et al. 2007; Jeřábková et al. 2018 for a discussion of this limit). Details of the IGIMF calculations can be found in Jeřábková et al. (2018). We define the correction factor (eq. 17 in Jeřábková et al. 2018),

$$\Psi = \frac{SFR_{\text{K or SLUG or IGIMF}}}{SFR_{\text{K}}}.$$
 (1.17)

Assuming the IMF is a PDF (Sec. 1.6.1, point 1), the average over an ensemble of galaxies with the same baryonic mass, $\overline{\Psi}=1$, for all $SFR_{\rm K}$ with increasing scatter as $SFR_{\rm K}$ decreases. The scatter in $SFR_{\rm K}$ will constitute a few orders of magnitude for $SFR_{\rm true} \lesssim 0.1\,M_{\odot}/{\rm yr}$ as a result of randomly sampling stars from the IMF without constraints. For example, there can be galaxies which contain no ionising stars (such that $SFR_{\rm K}\approx 0\,M_{\odot}/{\rm yr}$) despite having $SFR_{\rm true}=1\,M_{\odot}/{\rm yr}$. Alternatively, there can be galaxies consisting only of ionising stars and with the same $SFR_{\rm true}$.

In the SLUG approach (Sec. 1.6.1, point 2), $\overline{\Psi} > 1$ for $SFR_{\rm true} \lesssim 1\,M_{\odot}/{\rm yr}$, increasing with decreasing $SFR_{\rm K}$. For decreasing $SFR_{\rm true}$, the scatter in $SFR_{\rm K}$ increases up to a few orders of magnitude. For $SFR_{\rm true} \gtrsim 1\,M_{\odot}/{\rm yr}$, $\overline{\Psi} = 1$ (fig. 2 in da Silva et al. 2014). The reason for this comes about because at low $SFR_{\rm true}$, the galaxy is populated typically with less-massive embedded clusters such that the gwIMF is not fully sampled to the highest allowed stellar masses. As a consequence, the true SFR, $SFR_{\rm true}$, is larger than that measured from the H α flux assuming the gwIMF is invariant and fully sampled (in this case $SFR_{\rm K}$) because the gwIMF contains fewer ionising stars per low-mass star. The scatter comes about because the IMF and ECMF are assumed to be PDFs (the IMF is a constrained PDF, the

constraint being that the random drawing of stars from the IMF must add up to the mass of the pre-determined embedded cluster, $M_{\rm ecl}$). Thus, in the SLUG approach it is possible to generate a galaxy which has no ionising stars despite having $SFR_{\rm true}=1\,M_{\odot}/{\rm yr}$. In the SLUG approach it is possible that a galaxy with $SFR_{\rm true}=1\times10^{-4}\,M_{\odot}/{\rm yr}$ forms only a single $10\,M_{\odot}$ star which needs this SFR ($10\,M_{\odot}$ being assembled in $10^5\,{\rm yr}$). In this case an observer would however conclude that $SFR_{\rm K}\gg10^{-4}\,M_{\odot}/{\rm yr}$ since the H α flux would be associated with a full gwIMF (modelled via the Kennicutt IMF). This is, by the way, also true for the pure stochastic approach above, such that there Ψ varies both sides of the value of one.

In the IGIMF approach (Sec. 1.4.2) galaxies always form populations of stars and these do not contain O stars when $SFR_{\rm true} < 10^{-4} \, M_{\odot}/{\rm yr}$ (table 3 in Weidner et al. 2013b, fig. 7 in Yan et al. 2017). This has led, in the literature, to confusion, since claims were made that observed galaxies with $SFR_{\rm K} < 10^{-4} \, M_{\odot}/{\rm yr}$ are producing O stars therewith ruling out the IGIMF theory. But these claims forgot that $\Psi \gg 1$ in these cases according to the IGIMF theory (see discussion of this in Jeřábková et al. 2018). It is evident from Figs. 1.5 and 1.6 that the number of ionising stars relative to the number of low-mass stars decreases systematically with decreasing $SFR_{\rm true}$. Consequently, $\Psi > 1$ for $SFR_{\rm K} \lesssim 1 \, M_{\odot}/{\rm yr}$, increasing with decreasing $SFR_{\rm K}$. This is a similar but stronger effect than in the SLUG approach. If the IMF is invariant and canonical, then $\Psi = 1$ for $SFR_{\rm K} \gtrsim 1 \, M_{\odot}/{\rm yr}$, as in the SLUG approach, which also assumes (in the current published version and in the spirit of the IMF being a PDF, i.e. not being subject to physical limits apart from the constraint given by $M_{\rm ecl}$ when drawing stars) that the IMF is invariant. In the IGIMF theory, the IMF is however assumed to systematically vary with the physical conditions of the molecular cloud (Eqs 1.8 and 1.9) such that $\Psi < 1$ for $SFR_{\rm K} \gtrsim 1 M_{\odot}/{\rm yr}$.

Kennicutt and Evans (2012) discuss the differences of these approaches and conclude that the systematic deviations observed between $SFR_{H\alpha}$ and SFR_{UV} (which is a reasonably good approximation of SFR_{true} , Pflamm-Altenburg et al. 2009) at small values of the SFR can be produced instead through temporal variations in SFRs, without having to resort to modifying the IMF. The galaxies would, however, need to be in an unexplained synchronised lull of their SFRs. Even if this were the correct conclusion, it would not be able to accommodate the systematic variation observed at high SFRs, which appear to merely be a natural continuation of the overall trend of the observationally-constrained gwIMF becoming increasingly top-heavy with increasing galaxy-wide SFR, beginning with a significantly top-light gwIMF in the least-massive dwarf galaxies (Fig. 1.6).

The above discussion is quantified in Fig. 1.7 which plots Ψ for the IGIMF case (the pure PDF case, point 1 in Sec. 1.4.1, has $\overline{\Psi} = 1$ independently of $SFR_{\rm K}$ with a scatter which is comparable to that evident in the SLUG case) and in fig. 3 in da Silva et al. (2014) for the SLUG approach.

1.7.1 The main sequence of galaxies

The vast majority (≈ 97 per cent) of galaxies with a baryonic mass larger than about $10^{10} M_{\odot}$ are disk galaxies today and $t \approx 6 \,\mathrm{Gyr}$ ago (Delgado-Serrano et al., 2010). These lie on a main sequence according to which the galaxy-wide stellar mass, M_* , correlates strongly with the SFR (Speagle et al., 2014). The SFR tracers employed are mostly sensitive to the luminous massive (ionising) stellar population in the galaxies and it was assumed that the gwIMF is invariant. Given the above correction factors (Eq. 1.17, Fig. 1.7), we can investigate how these affect the galaxy main sequence. We correct each $SFR_{\rm K}$ to obtain a new main sequence, under the assumption that the IGIMF3 model is valid and on assuming $SFR_{Speagle} = SFR_{K}$. This new main sequence and its dependence with redshift (assuming, as in Speagle et al. 2014, that the standard LCDM cosmological model applies) is shown in Fig 1.8. It transpires that the change of the SFR_{true} values, at a given baryonic galaxy mass, from z = 3 until today is reduced to an order of magnitude in comparison to two orders of magnitude according to Speagle et al. (2014). The slope is also lessened. Further work on how the gwIMF variation and a possibly different cosmological model (giving different luminosity and angular diameter distances) affect the true physical main sequence at different redshifts is required before firm conclusions can be reached on the true cosmological evolution of the main sequence. Since on a time-scale $\gtrsim 2.5\,\mathrm{Gyr}$ (Pflamm-Altenburg and Kroupa, 2009) the SFR needs to be up-kept by gas accretion, it follows that the gas-accretion rate is proportional to the stellar mass of the galaxy.

1.8 Conclusion

The relation of the IMF to the composite and the galaxy-wide IMF has been discussed. The mathematical treatment of the IMF (as a probability distribution function or an optimal distribution function) is closely associated with the physical processes according to which the distribution of stellar masses emerges from the interstellar medium. Three types of possibilities are being discussed and investigated in the community, and these lead to different predictions on the relation between the tracer used to asses the star

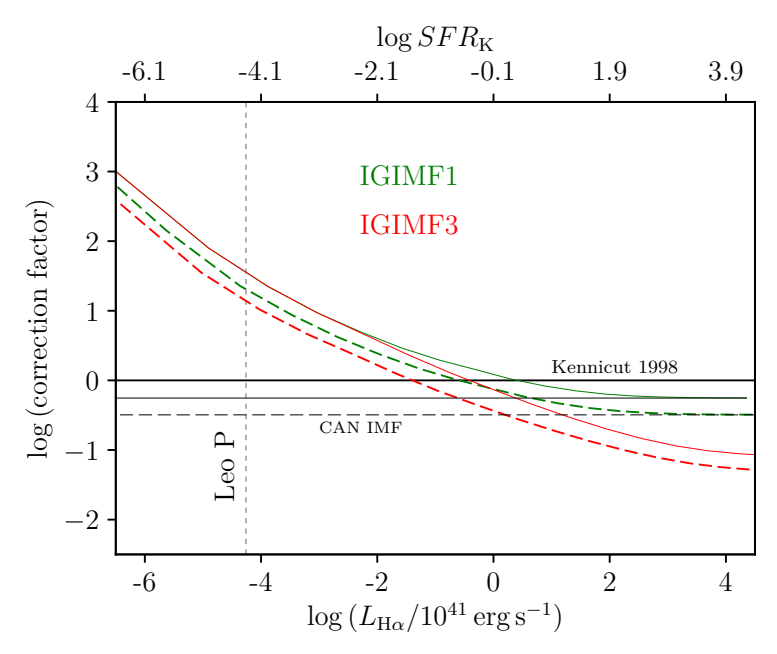


Figure 1.7 The correction factor Ψ (Eq. 1.17, $\log x \equiv \log_{10} x$ for any x) is plotted for various cases: the horizontal solid line is $\Psi = 1$ whereby the gwIMF used by Kennicutt (1998) is assumed, the thin solid and dashed horizontal lines are for an invariant canonical IMF (Eq. 1.1) for [Fe/H]= 0 and -2, respectively. The solid green and red curves are IGIMF models for [Fe/H] = 0 assuming, respectively, the IMF varies only through α_3 (Eq. 1.9, "IGIMF1") or ("IGIMF3" which is the most realistic case) at the low-mass end (Eq. 1.8) and at the high-mass end (Eq. 1.9). The corresponding dashed lines are for [Fe/H] = -2. Note that for [Fe/H] = 0 IGIMF1 and IGIMF3 bifurcate for $SFR \gtrsim 10^{-1.5} M_{\odot}/\text{yr}$ because the IMFs are identical to the canonical IMF at the low mass end at this metallicity, while at [Fe/H] = -2the IGIMF1 and IGIMF3 models remain separated at all SFRs because the IMFs differ at the low- and at the high-mass end at this metallicity. Thus, for example taking the case of a dwarf galaxy with [Fe/H] = -2 and measured $SFR_{\rm K} \approx 10^{-4.2}\,M_{\odot}/{\rm yr}$, it would have, according to the IGIMF3 model $SFR_{\rm true} \approx \Psi \times 10^{-4.2}\,M_{\odot}/{\rm yr}$ with $\Psi \approx 10^{1.2}$. A massive disk galaxy with [Fe/H]= 0 and $SFR_{\rm K} \approx 10^{1.9}\,M_{\odot}/{\rm yr}$ would have a $\Psi \approx 10^{-0.7}$ times larger $SFR_{\rm true}$. If the IGIMF theory is applicable, then the Leo P dwarf galaxy has a $SFR_{\rm true} \approx \Psi \times 10^{-4.2}\,M_{\odot}/{\rm yr}$ with $\Psi \approx 10^{1.2}$ explaining why it has one or two O stars. The presence of these stars has been leading to confusion in the literature if the $SFR_{
m K}$ value for its SFR is assumed (McQuinn et al., 2015). Adapted from Jeřábková et al. (2018).

formation rate of a galaxy, e.g. $SFR_{H\alpha}$, and the true star formation rate, $SFR_{\rm true}$. The H α and FUV flux is often employed to assess the SFR (over the past ≈ 50 and 400 Myr, respectively) and we used the former as an example to show the differences in the predictions. Assuming in all cases that

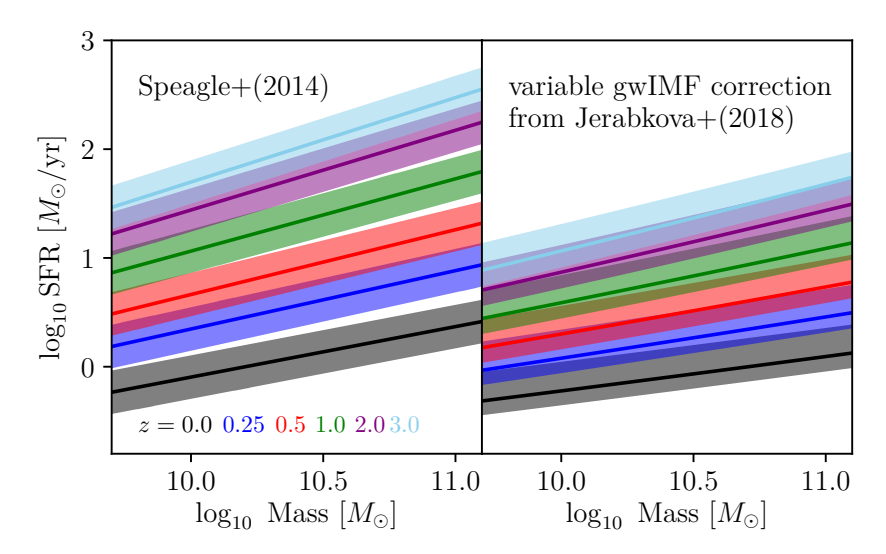


Figure 1.8 The galaxy main sequence according to which the true SFR of a galaxy (on the y-axis) depends on the stellar mass, M_* (on the x axis) of the galaxy. The **left panel** shows the original quantification by Speagle et al. (2014) with the colour coding according to redshift, z, as indicated at the bottom of the panel. The **right panel** shows the new main sequence after applying the correction factor Ψ (Eq. 1.17, Fig. 1.7) assuming the IGIMF3 model. Assuming the correction factors to be correct, the new main sequence would have a shallower slope, the SFRs would be lower and the evolution with redshift would be reduced. This is a consequence of the gwIMF depending on the metallicity and SFR, which is driven by the IMF becoming top-heavy in star-burst star clusters.

dust obscuration, photon leakage and other effects (Calzetti, 2008, 2013) do not play a role, and that the SFR does not vary over time-scales of less than about 50 Myr:

1. If the IMF is a pure PDF without constraints apart from the possible existence of an upper mass limit to stars $(m_{\text{max*}}, \text{ Sec. } 1.6.1)$ then $SFR_{\text{H}\alpha}$ is an unbiased tracer of SFR $(SFR_{\text{H}\alpha} \propto SFR_{\text{true}})$ and the dispersion of the SFRs, $\sigma_{SFR(\text{H}\alpha)}$, increases with decreasing SFR_{true} due to stochastic variations. This dispersion can be orders of magnitude, since galaxies can be sampled which have no ionising stars or which consist only of ionising stars. This model cannot reproduce the observed systematic trend of the gwIMF becoming increasingly top-light with decreasing $SFR_{\text{true}} \lesssim 1 \, M_{\odot}/\text{yr}$, nor the observed systematic trend of the gwIMF becoming increasingly top-heavy with increasing $SFR_{\text{true}} \gtrsim 1 \, M_{\odot}/\text{yr}$ (Fig. 1.6), nor the $m_{\text{max}} - M_{\text{ecl}}$ data (Fig. 1.3). If a galaxy has an observed

- 46 The initial mass function of stars and the star-formation rates of galaxies $H\alpha$ flux, then this approach does not allow the determination of $SFR_{\rm true}$
 - $H\alpha$ flux, then this approach does not allow the determination of SFR_{true} unless one is in the regime where $\sigma_{SFR(H\alpha)}$ is sufficiently small.
- 2. If it is assumed that stars from in embedded clusters which are drawn stochastically from the ECMF and that the IMF is sampled stochastically within each embedded cluster with the constraint that $M_{\rm ecl}$ be fulfilled (the SLUG approach, Sec. 1.6.1), then $SFR_{\rm H\alpha}$ increasingly underestimates SFR_{true} with decreasing $SFR_{\text{true}} \lesssim 1 M_{\odot}/\text{yr}$. The dispersion, $\sigma_{SFR(H\alpha)}$, also increases with decreasing SFR_{true} due to stochastic variations, but to a lesser extend than under point 1, since the constraint $M_{
 m ecl}$ limits the possible variations. This model allows for galaxies to contain no ionising stars and also for galaxies to consist only of ionising stars and so $\sigma_{SFR(H\alpha)}$ reaches orders of magnitude at low SFR_{true} (da Silva et al., 2014). This model can approximately reproduce the observed systematic trend of the gwIMF becoming increasingly top-light with decreasing SFR_{true} (da Silva et al. 2014, Fig. 1.6, Eq. 1.17, Fig. 1.7), but not the $m_{\rm max} - M_{\rm ecl}$ data (Fig. 1.3). It can also not reproduce the observed systematic trend of the gwIMF becoming increasingly top-heavy with increasing $SFR_{\rm true} \gtrsim 1 \, M_{\odot}/{\rm yr}$ (Fig. 1.6). If a galaxy has an observed $H\alpha$ flux, then this approach does not allow the determination of SFR_{true} unless one is in the regime where $\sigma_{SFR(H\alpha)}$ is sufficiently small.
- 3. If the IGIMF theory is assumed, then $SFR_{H\alpha}$ increasingly underestimates $SFR_{\rm true}$ with decreasing $SFR_{\rm true} \lesssim 1 \, M_{\odot}/{\rm yr}$ with a somewhat larger systematic change than under point 2. A small dispersion, $\sigma_{SFR(H\alpha)}$, at small SFR is present due to the birth and death of individual most-massive stars in the galaxy. Since galaxies are interacting and have internal dynamical instabilities which affect the assembly of molecular clouds (e.g., the bar instability), a natural $\sigma_{SFR(H\alpha)}$ will be observable, but this has not yet been calculated. This model can reproduce the observed systematic trend of the gwIMF becoming increasingly top-light with decreasing SFR_{true} (Lee et al. 2009, Fig. 1.6, Eq. 1.17, Fig. 1.7) and the $m_{\rm max} - M_{\rm ecl}$ data (Fig. 1.3). It can also reproduce the observed systematic trend of the gwIMF becoming increasingly top-heavy with increasing $SFR_{\rm true} \gtrsim 1 \, M_{\odot}/{\rm yr}$ (Fig. 1.6) due to the incorporation of the metallicity and density dependent IMF (Eq. 1.8 and 1.9). If a galaxy has an observed $H\alpha$ flux, then this approach provides a unique determination of SFR_{true} , since the expected variation, $\sigma_{SFR(H\alpha)}$, for galaxies of the same baryonic mass can (we expect) be related to the distribution of morphologies of the galaxies and there is no stochasticity.

Efficient IMF-sampling algorithms are available as downloads: for stochas-

tic sampling see Pflamm-Altenburg and Kroupa (2006) and Kroupa et al. (2013) and for optimal sampling see Yan et al. (2017) and Kroupa et al. (2013). For the SLUG approach (relevant for points 1 and 2 in Sec. 1.6.1) programs are available (da Silva et al., 2012, 2014; Ashworth et al., 2017), while for the IGIMF approach also (Yan et al., 2017; Jeřábková et al., 2018).

The IGIMF theory has been computed with and without a variable IMF, and the most realistic case is IGIMF3 (Jeřábková et al., 2018) which incorporates the full IMF dependency on density and metallicity (Eq. 1.8 and 1.9) currently known from observational data. The two stochastic approaches above (points 1 and 2 in Sec. 1.6.1) may be used with a variable IMF also. But an IMF which varies systematically with physical conditions may be in tension with an interpretation of the IMF as a PDF since it implies that conditions need to be applied on the PDF. If the IMF becomes top-heavy at high SFR density (e.g. as formulated in Eq. 1.9) then galaxies with a $SFR_{\rm true} \gtrsim 1\,M_{\odot}/{\rm yr}$ will have $SFR_{\rm H\alpha}$ overestimating $SFR_{\rm true}$, just as in the IGIMF theory.

The observational constraints (Boxes I–IV, p. 16, 24,30, 35) are useful for assessing which of the above possibilities are relevant for nature: The existence or not existence of isolated massive stars and of a physical $m_{\rm max}-M_{\rm ecl}$ relation (Fig. 1.3) and its dispersion are thus central issues in understanding SFR measurements of galaxies. Important for the interpretation of the IMF and thus on how to compute gwIMFs and galaxy-wide SFRs given some tracer is also whether embedded clusters can be viewed as being fundamental building blocks of galaxies (Kroupa, 2005) and if stars form mass segregated in these embedded clusters. If this is the case, then it is also important if the ECMF varies systematically within a galaxy, e.g. radially. To further clarify these points, which all play a role in our interpretation of the IMF and its relation to the cIMF and gwIMF, further observational work is required. But that these issues are being discussed shows how rich and informative this topic is. An important constraint on any formulation of the gwIMF is that this formulation must be consistent with the IMFs deduced from resolved stellar populations (star clusters, stellar associations). The implications for our understanding of how galaxies evolve are potentially major, as discussed in this contribution. Certainly, as an example, the quantification of the main sequence of galaxies depends on how we understand the gwIMF (Sec. 1.7.1).

Returning to elliptical galaxies (Box Observational Constraint IV, page 35), the need for a bottom-heavy and a top-heavy gwIMF, possibly in terms of the evolution of the gwIMF, is a challenge for any theory of how elliptical galaxies formed and evolved (Weidner et al., 2013a; Ferreras et al., 2015; Jeřábková et al., 2018). It is clear that elliptical galaxies are unusual, mak-

ing only a few per cent of the population of galaxies heavier than about $10^{10}\,M_\odot$ (Delgado-Serrano et al., 2010), and that elliptical galaxies formed rapidly and thus with $SFR_{\rm true} > 1000\,M_\odot/{\rm yr}$. Any such theory needs to be consistent with the data on star-forming galaxies. Important in this context are the constraints on the allowed dark matter (faint M dwarfs, stellar remnants) from lensing observations (Smith and Lucey, 2013; Smith, 2014) which appear to be inconsistent with the bottom-heavy gwIMF to provide a significant amount of mass. This problem is discussed also in the review on elliptical galaxies by Cappellari (2016) and significantly advanced by Yan et al. (2021).

References

- Adams, F. C., and Fatuzzo, M. 1996. A Theory of the Initial Mass Function for Star Formation in Molecular Clouds. ApJ, 464(June), 256.
- André, P., Men'shchikov, A., Bontemps, S., Könyves, V., Motte, F., Schneider, N., Didelon, P., Minier, V., Saraceno, P., Ward-Thompson, D., di Francesco, J., White, G., Molinari, S., Testi, L., Abergel, A., Griffin, M., Henning, T., Royer, P., Merín, B., Vavrek, R., Attard, M., Arzoumanian, D., Wilson, C. D., Ade, P., Aussel, H., Baluteau, J.-P., Benedettini, M., Bernard, J.-P., Blommaert, J. A. D. L., Cambrésy, L., Cox, P., di Giorgio, A., Hargrave, P., Hennemann, M., Huang, M., Kirk, J., Krause, O., Launhardt, R., Leeks, S., Le Pennec, J., Li, J. Z., Martin, P. G., Maury, A., Olofsson, G., Omont, A., Peretto, N., Pezzuto, S., Prusti, T., Roussel, H., Russeil, D., Sauvage, M., Sibthorpe, B., Sicilia-Aguilar, A., Spinoglio, L., Waelkens, C., Woodcraft, A., and Zavagno, A. 2010. From filamentary clouds to prestellar cores to the stellar IMF: Initial highlights from the Herschel Gould Belt Survey. A&A, 518(July), L102.
- André, P., Di Francesco, J., Ward-Thompson, D., Inutsuka, S.-I., Pudritz, R. E., and Pineda, J. E. 2014. From Filamentary Networks to Dense Cores in Molecular Clouds: Toward a New Paradigm for Star Formation. *Protostars and Planets VI*, 27–51.
- Andrews, J. E., Calzetti, D., Chandar, R., Lee, J. C., Elmegreen, B. G., Kennicutt, R. C., Whitmore, B., Kissel, J. S., da Silva, R. L., Krumholz, M. R., O'Connell, R. W., Dopita, M. A., Frogel, J. A., and Kim, H. 2013. An Initial Mass Function Study of the Dwarf Starburst Galaxy NGC 4214. *ApJ*, **767**(Apr.), 51
- Andrews, J. E., Calzetti, D., Chandar, R., Elmegreen, B. G., Kennicutt, R. C., Kim, H., Krumholz, M. R., Lee, J. C., McElwee, S., O'Connell, R. W., and Whitmore, B. 2014. Big Fish in Small Ponds: Massive Stars in the Low-mass Clusters of M83. *ApJ*, **793**(Sept.), 4.
- Applebaum, Elaad, Brooks, Alyson M., Quinn, Thomas R., and Christensen, Charlotte R. 2020. A stochastically sampled IMF alters the stellar content of simulated dwarf galaxies. *MNRAS*, **492**(1), 8–21.
- Ashworth, G., Fumagalli, M., Krumholz, M. R., Adamo, A., Calzetti, D., Chandar, R., Cignoni, M., Dale, D., Elmegreen, B. G., Gallagher, III, J. S., Gouliermis, D. A., Grasha, K., Grebel, E. K., Johnson, K. E., Lee, J., Tosi, M., and Wofford, A. 2017. Exploring the IMF of star clusters: a joint SLUG and LEGUS effort. MNRAS, 469(Aug.), 2464–2480.

- Ballero, S. K., Kroupa, P., and Matteucci, F. 2007. Testing the universal stellar IMF on the metallicity distribution in the bulges of the Milky Way and M 31. $A \mathcal{E} A$, 467(May), 117–121.
- Banerjee, S., and Kroupa, P. 2012. On the true shape of the upper end of the stellar initial mass function. The case of R136. A &A, 547(Nov.), A23.
- Banerjee, S., and Kroupa, P. 2017. How can young massive clusters reach their present-day sizes? $A \mathcal{C}A$, 597(Jan.), A28.
- Banerjee, S., Kroupa, P., and Oh, S. 2012. The emergence of super-canonical stars in R136-type starburst clusters. *MNRAS*, **426**(Oct.), 1416–1426.
- Bastian, N., Covey, K. R., and Meyer, M. R. 2010. A Universal Stellar Initial Mass Function? A Critical Look at Variations. ARA &A, 48(Sept.), 339–389.
- Bate, M. R. 2005. The dependence of the initial mass function on metallicity and the opacity limit for fragmentation. *MNRAS*, **363**(Oct.), 363–378.
- Bate, M. R. 2014. The statistical properties of stars and their dependence on metallicity: the effects of opacity. MNRAS, 442(July), 285–313.
- Bate, M. R., Bonnell, I. A., and Bromm, V. 2002. The formation mechanism of brown dwarfs. MNRAS, 332(May), L65–L68.
- Bate, M. R., Tricco, T. S., and Price, D. J. 2014. Collapse of a molecular cloud core to stellar densities: stellar-core and outflow formation in radiation magnetohydrodynamic simulations. *MNRAS*, **437**(Jan.), 77–95.
- Baumgardt, H., and Makino, J. 2003. Dynamical evolution of star clusters in tidal fields. *MNRAS*, **340**(Mar.), 227–246.
- Baumgardt, H., De Marchi, G., and Kroupa, P. 2008. Evidence for Primordial Mass Segregation in Globular Clusters. *ApJ*, **685**(Sept.), 247–253.
- Belloni, D., Askar, A., Giersz, M., Kroupa, P., and Rocha-Pinto, H. J. 2017. On the initial binary population for star cluster simulations. *MNRAS*, **471**(Nov.), 2812–2828.
- Belloni, D., Kroupa, P., Rocha-Pinto, H. J., and Giersz, M. 2018. Dynamical equivalence, the origin of the Galactic field stellar and binary population, and the initial radius-mass relation of embedded clusters. *MNRAS*, **474**(Mar.), 3740–3745.
- Bertelli Motta, C., Clark, P. C., Glover, S. C. O., Klessen, R. S., and Pasquali, A. 2016. The IMF as a function of supersonic turbulence. *MNRAS*, **462**(Nov.), 4171–4182.
- Beuther, H., Churchwell, E. B., McKee, C. F., and Tan, J. C. 2007 (Jan.). The Formation of Massive Stars. Page 165 of: Reipurth, Bo, Jewitt, David, and Keil, Klaus (eds), *Protostars and Planets V*.
- Boissier, S., Gil de Paz, A., Boselli, A., Madore, B. F., Buat, V., Cortese, L., Burgarella, D., Muñoz-Mateos, J. C., Barlow, T. A., Forster, K., Friedman, P. G., Martin, D. C., Morrissey, P., Neff, S. G., Schiminovich, D., Seibert, M., Small, T., Wyder, T. K., Bianchi, L., Donas, J., Heckman, T. M., Lee, Y.-W., Milliard, B., Rich, R. M., Szalay, A. S., Welsh, B. Y., and Yi, S. K. 2007. Radial Variation of Attenuation and Star Formation in the Largest Late-Type Disks Observed with GALEX. ApJS, 173(Dec.), 524–537.
- Bonnell, I. A., and Davies, M. B. 1998. Mass segregation in young stellar clusters. *MNRAS*, **295**(Apr.), 691.
- Bontemps, S., Motte, F., Csengeri, T., and Schneider, N. 2010. Fragmentation and mass segregation in the massive dense cores of Cygnus X. $A \mathcal{E} A$, **524**(Dec.), A18.

- Breitschwerdt, D., de Avillez, M. A., Feige, J., and Dettbarn, C. 2012. Interstellar medium simulations. *Astronomische Nachrichten*, **333**(June), 486.
- Brinkmann, N., Banerjee, S., Motwani, B., and Kroupa, P. 2017. The bound fraction of young star clusters. $A \mathcal{C}A$, **600**(Apr.), A49.
- Burkert, A. 2006. The turbulent interstellar medium. Comptes Rendus Physique, 7(Apr.), 433–441.
- Calzetti, D. 2008 (June). Star Formation Rate Determinations. Page 121 of: Knapen, J. H., Mahoney, T. J., and Vazdekis, A. (eds), Pathways Through an Eclectic Universe. Astronomical Society of the Pacific Conference Series, vol. 390.
- Calzetti, D. 2013. Star Formation Rate Indicators. Page 419.
- Cappellari, M. 2016. Structure and Kinematics of Early-Type Galaxies from Integral Field Spectroscopy. ARA&A, **54**(Sept.), 597–665.
- Cerviño, M., Román-Zúñiga, C., Luridiana, V., Bayo, A., Sánchez, N., and Pérez, E. 2013a. Crucial aspects of the initial mass function. I. The statistical correlation between the total mass of an ensemble of stars and its most massive star. $A \mathcal{C} A$, 553(May), A31.
- Cerviño, M., Román-Zúñiga, C., Bayo, A., Luridiana, V., Sánchez, N., and Pérez, E. 2013b. Crucial aspects of the initial mass function. II. The inference of total quantities from partial information on a cluster. $A \mathcal{E} A$, 553(May), A32.
- Chabrier, G. 2003. Galactic Stellar and Substellar Initial Mass Function. *PASP*, **115**(July), 763–795.
- Chené, A.-N., Ramírez Alegría, S., Borissova, J., O'Leary, E., Martins, F., Hervé, A., Kuhn, M., Kurtev, R., Consuelo Amigo Fuentes, P., Bonatto, C., and Minniti, D. 2015. Massive open star clusters using the VVV survey. IV. WR 62-2, a new very massive star in the core of the VVV CL041 cluster. $A \mathcal{E} A$, $584(\mathrm{Dec.})$, A31.
- Concas, A., Popesso, P., Brusa, M., Mainieri, V., Erfanianfar, G., and Morselli, L. 2017. Light breeze in the local Universe. $A \mathcal{C}A$, **606**(Oct.), A36.
- Conroy, C., and van Dokkum, P. G. 2012. The Stellar Initial Mass Function in Early-type Galaxies From Absorption Line Spectroscopy. II. Results. ApJ, **760**(Nov.), 71.
- Crowther, P. A., Schnurr, O., Hirschi, R., Yusof, N., Parker, R. J., Goodwin, S. P., and Kassim, H. A. 2010. The R136 star cluster hosts several stars whose individual masses greatly exceed the accepted 150M_{solar} stellar mass limit. MNRAS, 408(Oct.), 731–751.
- da Silva, R. L., Fumagalli, M., and Krumholz, M. 2012. SLUG: Stochastically Lighting Up Galaxies. I. Methods and Validating Tests. ApJ, 745(Feb.), 145.
- da Silva, R. L., Fumagalli, M., and Krumholz, M. R. 2014. SLUG Stochastically Lighting Up Galaxies II. Quantifying the effects of stochasticity on star formation rate indicators. *MNRAS*, 444(Nov.), 3275–3287.
- Dabringhausen, J., Kroupa, P., and Baumgardt, H. 2009. A top-heavy stellar initial mass function in starbursts as an explanation for the high mass-to-light ratios of ultra-compact dwarf galaxies. *MNRAS*, **394**(Apr.), 1529–1543.
- Dabringhausen, J., Fellhauer, M., and Kroupa, P. 2010. Mass loss and expansion of ultra compact dwarf galaxies through gas expulsion and stellar evolution for top-heavy stellar initial mass functions. *MNRAS*, **403**(Apr.), 1054–1071.
- Dabringhausen, J., Kroupa, P., Pflamm-Altenburg, J., and Mieske, S. 2012. Low-mass X-Ray Binaries Indicate a Top-heavy Stellar Initial Mass Function in Ultracompact Dwarf Galaxies. *ApJ*, **747**(Mar.), 72.

- de Mink, S. E., Sana, H., Langer, N., Izzard, R. G., and Schneider, F. R. N. 2014. The Incidence of Stellar Mergers and Mass Gainers among Massive Stars. ApJ, **782**(Feb.), 7.
- Delgado-Serrano, R., Hammer, F., Yang, Y. B., Puech, M., Flores, H., and Rodrigues, M. 2010. How was the Hubble sequence 6 Gyr ago? $A \mathcal{C}A$, 509(Jan.), A78.
- Dib, S. 2014. Testing the universality of the IMF with Bayesian statistics: young clusters. *MNRAS*, **444**(Oct.), 1957–1981.
- Dib, S., Kim, J., and Shadmehri, M. 2007. The origin of the Arches stellar cluster mass function. *MNRAS*, **381**(Oct.), L40–L44.
- Dib, S., Schmeja, S., and Hony, S. 2017. Massive stars reveal variations of the stellar initial mass function in the Milky Way stellar clusters. MNRAS, 464(Jan.), 1738–1752.
- Disney, M. J., Romano, J. D., Garcia-Appadoo, D. A., West, A. A., Dalcanton, J. J., and Cortese, L. 2008. Galaxies appear simpler than expected. *Nature*, **455**(Oct.), 1082–1084.
- Duarte-Cabral, A., Bontemps, S., Motte, F., Hennemann, M., Schneider, N., and André, P. 2013. CO outflows from high-mass Class 0 protostars in Cygnus-X. $A \mathcal{B} A$, 558(Oct.), A125.
- Egusa, F., Sofue, Y., and Nakanishi, H. 2004. Offsets between $H\alpha$ and CO Arms of a Spiral Galaxy, NGC 4254: A New Method for Determining the Pattern Speed of Spiral Galaxies. *PASJ*, **56**(Dec.), L45–L48.
- Egusa, F., Kohno, K., Sofue, Y., Nakanishi, H., and Komugi, S. 2009. Determining Star Formation Timescale and Pattern Speed in Nearby Spiral Galaxies. *ApJ*, **697**(June), 1870–1891.
- Egusa, F., Mentuch Cooper, E., Koda, J., and Baba, J. 2017. Gas and stellar spiral arms and their offsets in the grand-design spiral galaxy M51. *MNRAS*, **465**(Feb.), 460–471.
- Elmegreen, B. G. 1997. The Initial Stellar Mass Function from Random Sampling in a Turbulent Fractal Cloud. *ApJ*, **486**(Sept.), 944–954.
- Elmegreen, B. G. 1999. The Stellar Initial Mass Function from Random Sampling in Hierarchical Clouds. II. Statistical Fluctuations and a Mass Dependence for Starbirth Positions and Times. *ApJ*, **515**(Apr.), 323–336.
- Elmegreen, B. G. 2000. Modeling a High-Mass Turn-Down in the Stellar Initial Mass Function. ApJ, **539**(Aug.), 342–351.
- Elmegreen, B. G. 2004. Variability in the stellar initial mass function at low and high mass: three-component IMF models. MNRAS, **354**(Oct.), 367–374.
- Elmegreen, B. G., and Scalo, J. 2006. The Effect of Star Formation History on the Inferred Stellar Initial Mass Function. ApJ, **636**(Jan.), 149–157.
- Federrath, C. 2015. Inefficient star formation through turbulence, magnetic fields and feedback. MNRAS, 450(July), 4035–4042.
- Federrath, C. 2016. On the universality of interstellar filaments: theory meets simulations and observations. *MNRAS*, **457**(Mar.), 375–388.
- Federrath, C., Schrön, M., Banerjee, R., and Klessen, R. S. 2014. Modeling Jet and Outflow Feedback during Star Cluster Formation. *ApJ*, **790**(Aug.), 128.
- Ferreras, I., Weidner, C., Vazdekis, A., and La Barbera, F. 2015. Further evidence for a time-dependent initial mass function in massive early-type galaxies. MN-RAS, 448(Mar.), L82–L86.
- Figer, D. F. 2005. An upper limit to the masses of stars. $Nature, \, 434 (Mar.), \, 192-194.$

- Fukui, Y., and Kawamura, A. 2010. Molecular Clouds in Nearby Galaxies. *ARA&A*, **48**(Sept.), 547–580.
- Fumagalli, M., da Silva, R. L., and Krumholz, M. R. 2011. Stochastic Star Formation and a (Nearly) Uniform Stellar Initial Mass Function. ApJ, 741(Nov.), L26.
- Garcia, Miriam, Herrero, Artemio, Najarro, Francisco, Camacho, Inés, and Lorenzo, Marta. 2019. Ongoing star formation at the outskirts of Sextans A: spectroscopic detection of early O-type stars. MNRAS, 484(1), 422–430.
- Gargiulo, I. D., Cora, S. A., Padilla, N. D., Muñoz Arancibia, A. M., Ruiz, A. N., Orsi, A. A., Tecce, T. E., Weidner, C., and Bruzual, G. 2015. Chemoarchaeological downsizing in a hierarchical universe: impact of a top-heavy IGIMF. MNRAS, 446(Feb.), 3820–3841.
- Gieles, M., Moeckel, N., and Clarke, C. J. 2012. Do all stars in the solar neighbourhood form in clusters? A cautionary note on the use of the distribution of surface densities. *MNRAS*, **426**(Oct.), L11–L15.
- Goodwin, S. P., and Kroupa, P. 2005. Limits on the primordial stellar multiplicity. $A\mathcal{B}A$, $\mathbf{439}(\mathrm{Aug.})$, 565-569.
- Gunawardhana, M. L. P., Hopkins, A. M., Sharp, R. G., Brough, S., Taylor, E., Bland-Hawthorn, J., Maraston, C., Tuffs, R. J., Popescu, C. C., Wijesinghe, D., Jones, D. H., Croom, S., Sadler, E., Wilkins, S., Driver, S. P., Liske, J., Norberg, P., Baldry, I. K., Bamford, S. P., Loveday, J., Peacock, J. A., Robotham, A. S. G., Zucker, D. B., Parker, Q. A., Conselice, C. J., Cameron, E., Frenk, C. S., Hill, D. T., Kelvin, L. S., Kuijken, K., Madore, B. F., Nichol, B., Parkinson, H. R., Pimbblet, K. A., Prescott, M., Sutherland, W. J., Thomas, D., and van Kampen, E. 2011. Galaxy and Mass Assembly (GAMA): the star formation rate dependence of the stellar initial mass function. MNRAS, 415(Aug.), 1647–1662.
- Gvaramadze, V. V., Weidner, C., Kroupa, P., and Pflamm-Altenburg, J. 2012. Field O stars: formed in situ or as runaways? *MNRAS*, **424**(Aug.), 3037–3049.
- Hacar, A., Tafalla, M., Kauffmann, J., and Kovács, A. 2013. Cores, filaments, and bundles: hierarchical core formation in the L1495/B213 Taurus region. $A \mathcal{C}A$, **554**(June), A55.
- Hacar, A., Tafalla, M., and Alves, J. 2017a. Fibers in the NGC 1333 proto-cluster. $A \mathcal{C}A$, **606**(Oct.), A123.
- Hacar, A., Alves, J., Tafalla, M., and Goicoechea, J. R. 2017b. Gravitational collapse of the OMC-1 region. $A \mathcal{C}A$, **602**(June), L2.
- Haghi, H., Zonoozi, A. H., Kroupa, P., Banerjee, S., and Baumgardt, H. 2015. Possible smoking-gun evidence for initial mass segregation in re-virialized post-gas expulsion globular clusters. *MNRAS*, **454**(Dec.), 3872–3885.
- Haghi, H., Khalaj, P., Hasani Zonoozi, A., and Kroupa, P. 2017. A Possible Solution for the M/L-[Fe/H] Relation of Globular Clusters in M31. II. The Age-Metallicity Relation. ApJ, 839(Apr.), 60.
- Haugbølle, T., Padoan, P., and Nordlund, Å. 2018. The Stellar IMF from Isothermal MHD Turbulence. ApJ, **854**(Feb.), 35.
- Heggie, D., and Hut, P. 2003. The Gravitational Million-Body Problem: A Multidisciplinary Approach to Star Cluster Dynamics.
- Hennebelle, P., and Chabrier, G. 2013. Analytical Theory for the Initial Mass Function. III. Time Dependence and Star Formation Rate. ApJ, 770(June), 150.

- Henry, T. J., Jao, W.-C., Winters, J. G., Dieterich, S. B., Finch, C. T., Ianna, P. A.,
 Riedel, A. R., Silverstein, M. L., Subasavage, J. P., and Vrijmoet, E. H. 2018.
 The Solar Neighborhood XLIV: RECONS Discoveries within 10 parsecs. AJ,
 155(June), 265.
- Heyer, M., and Dame, T. M. 2015. Molecular Clouds in the Milky Way. ARA &A, 53(Aug.), 583–629.
- Hopkins, A. M. 2018. The Dawes Review 8: Measuring the Stellar Initial Mass Function. *PASA*, **35**(Nov.), e039.
- Hopkins, P. F. 2012. The stellar initial mass function, core mass function and the last-crossing distribution. *MNRAS*, **423**(July), 2037–2044.
- Hopkins, P. F. 2013a. Variations in the stellar CMF and IMF: from bottom to top. *MNRAS*, **433**(July), 170–177.
- Hopkins, P. F. 2013b. Why do stars form in clusters? An analytic model for stellar correlation functions. *MNRAS*, **428**(Jan.), 1950–1957.
- Hosek, Matthew W., Jr., Lu, Jessica R., Anderson, Jay, Najarro, Francisco, Ghez, Andrea M., Morris, Mark R., Clarkson, William I., and Albers, Saundra M. 2019. The Unusual Initial Mass Function of the Arches Cluster. ApJ, 870(1), 44.
- Hoversten, E. A., and Glazebrook, K. 2008. Evidence for a Nonuniversal Stellar Initial Mass Function from the Integrated Properties of SDSS Galaxies. ApJ, **675**(Mar.), 163–187.
- Hsu, W.-H., Hartmann, L., Allen, L., Hernández, J., Megeath, S. T., Mosby, G., Tobin, J. J., and Espaillat, C. 2012. The Low-mass Stellar Population in L1641: Evidence for Environmental Dependence of the Stellar Initial Mass Function. ApJ, **752**(June), 59.
- Jeřábková, T., Kroupa, P., Dabringhausen, J., Hilker, M., and Bekki, K. 2017. The formation of ultra compact dwarf galaxies and massive globular clusters. Quasar-like objects to test for a variable stellar initial mass function. $A \mathcal{C} A$, **608**(Dec.), A53.
- Jeřábková, T., Hasani Zonoozi, A., Kroupa, P., Beccari, G., Yan, Z., Vazdekis, A., and Zhang, Z. Y. 2018. Impact of metallicity and star formation rate on the time-dependent, galaxy-wide stellar initial mass function. $A \mathcal{C}A$, 620(Nov), A39.
- Joncour, Isabelle, Duchêne, Gaspard, Moraux, Estelle, and Motte, Frédérique. 2018. Multiplicity and clustering in Taurus star forming region. II. From ultra-wide pairs to dense NESTs. $A \mathcal{C}A$, **620**(Nov.), A27.
- Kalari, V. M., Carraro, G., Evans, C. J., and Rubio, M. 2018. The Magellanic Bridge Cluster NGC 796: Deep Optical AO Imaging Reveals the Stellar Content and Initial Mass Function of a Massive Open Cluster. *ApJ*, **857**(Apr.), 132.
- Kennicutt, R. C., and Evans, N. J. 2012. Star Formation in the Milky Way and Nearby Galaxies. $ARA \mathcal{C}A$, $\mathbf{50} (\mathrm{Sept.})$, 531–608.
- Kennicutt, Jr., R. C. 1989. The star formation law in galactic disks. ApJ, **344**(Sept.), 685–703.
- Kennicutt, Jr., R. C. 1998. The Global Schmidt Law in Star-forming Galaxies. ApJ, 498(May), 541–552.
- Kirk, H., and Myers, P. C. 2011. Young Stellar Groups and Their Most Massive Stars. *ApJ*, **727**(Feb.), 64.
- Kirk, H., and Myers, P. C. 2012. Variations in the Mass Functions of Clustered and Isolated Young Stellar Objects. *ApJ*, **745**(Feb.), 131.

- Kirk, H., Offner, S. S. R., and Redmond, K. J. 2014. The formation and evolution of small star clusters. *MNRAS*, **439**(Feb.), 1765–1780.
- Kirk, H., Johnstone, D., Di Francesco, J., Lane, J., Buckle, J., Berry, D. S.,
 Broekhoven-Fiene, H., Currie, M. J., Fich, M., Hatchell, J., Jenness, T., Mottram, J. C., Nutter, D., Pattle, K., Pineda, J. E., Quinn, C., Salji, C., Tisi, S.,
 Hogerheijde, M. R., Ward-Thompson, D., and The JCMT Gould Belt Survey
 Team. 2016. The JCMT Gould Belt Survey: Dense Core Clusters in Orion B.
 ApJ, 821(Apr.), 98.
- Koen, C. 2006. On the upper limit on stellar masses in the Large Magellanic Cloud cluster R136. MNRAS, **365**(Jan.), 590–594.
- Könyves, V., André, P., Men'shchikov, A., Palmeirim, P., Arzoumanian, D., Schneider, N., Roy, A., Didelon, P., Maury, A., Shimajiri, Y., Di Francesco, J., Bontemps, S., Peretto, N., Benedettini, M., Bernard, J.-P., Elia, D., Griffin, M. J., Hill, T., Kirk, J., Ladjelate, B., Marsh, K., Martin, P. G., Motte, F., Nguyên Luong, Q., Pezzuto, S., Roussel, H., Rygl, K. L. J., Sadavoy, S. I., Schisano, E., Spinoglio, L., Ward-Thompson, D., and White, G. J. 2015. A census of dense cores in the Aquila cloud complex: SPIRE/PACS observations from the Herschel Gould Belt survey. $A \mathcal{E}A$, 584(Dec.), A91.
- Köppen, J., Weidner, C., and Kroupa, P. 2007. A possible origin of the mass-metallicity relation of galaxies. *MNRAS*, **375**(Feb.), 673–684.
- Kristensen, L. E., and Dunham, M. M. 2018. Protostellar half-life: new methodology and estimates. $A \mathcal{E} A$, **618**(Oct.), A158.
- Kroupa, P. 1995a. Inverse dynamical population synthesis and star formation. *MNRAS*, **277**(Dec.), 1491.
- Kroupa, P. 1995b. The dynamical properties of stellar systems in the Galactic disc. MNRAS, **277**(Dec.).
- Kroupa, P. 1995c. Unification of the nearby and photometric stellar luminosity functions. ApJ, **453**(Nov.), 358.
- Kroupa, P. 2001. On the variation of the initial mass function. *MNRAS*, **322**(Apr.), 231–246.
- Kroupa, P. 2002a. The Initial Mass Function of Stars: Evidence for Uniformity in Variable Systems. *Science*, **295**(Jan.), 82–91.
- Kroupa, P. 2002b. Thickening of galactic discs through clustered star formation. $MNRAS, \, \bf 330 (Mar.), \, 707-718.$
- Kroupa, P. 2005 (Jan.). The Fundamental Building Blocks of Galaxies. Page 629 of: Turon, C., O'Flaherty, K. S., and Perryman, M. A. C. (eds), *The Three-Dimensional Universe with Gaia*. ESA Special Publication, vol. 576.
- Kroupa, P. 2008. Initial Conditions for Star Clusters. Page 181 of: Aarseth, S. J., Tout, C. A., and Mardling, R. A. (eds), *The Cambridge N-Body Lectures*. Lecture Notes in Physics, Berlin Springer Verlag, vol. 760.
- Kroupa, P., and Bouvier, J. 2003. The dynamical evolution of Taurus-Auriga-type aggregates. *MNRAS*, **346**(Dec.), 343–353.
- Kroupa, P., and Jerabkova, T. 2018. The Impact of Binaries on the Stellar Initial Mass Function. arXiv:1806.10605, June.
- Kroupa, P., and Weidner, C. 2003. Galactic-Field Initial Mass Functions of Massive Stars. ApJ, **598**(Dec.), 1076–1078.
- Kroupa, P., Gilmore, G., and Tout, C. A. 1991. The effects of unresolved binary stars on the determination of the stellar mass function. *MNRAS*, **251**(July), 293–302.

- Kroupa, P., Tout, C. A., and Gilmore, G. 1993. The distribution of low-mass stars in the Galactic disc. *MNRAS*, **262**(June), 545–587.
- Kroupa, P., Weidner, C., Pflamm-Altenburg, J., Thies, I., Dabringhausen, J., Marks, M., and Maschberger, T. 2013. The stellar and sub-stellar initial mass function of simple and composite populations. Page 115.
- Kroupa, P., Jeřábková, T., Dinnbier, F., Beccari, G., and Yan, Z. 2018. Evidence for feedback and stellar-dynamically regulated bursty star cluster formation: the case of the Orion Nebula Cluster. $A \mathcal{E} A$, **612**(Apr.), A74.
- Krumholz, M. R. 2014. The big problems in star formation: The star formation rate, stellar clustering, and the initial mass function. *Phys. Rep.*, **539**(June), 49–134.
- Krumholz, M. R. 2015. The Formation of Very Massive Stars. Page 43 of: Vink, J. S. (ed), Very Massive Stars in the Local Universe. Astrophysics and Space Science Library, vol. 412.
- Lada, C. J. 2010. The physics and modes of star cluster formation: observations. Philosophical Transactions of the Royal Society of London Series A, 368(Jan.), 713–731.
- Lada, C. J., and Lada, E. A. 2003. Embedded Clusters in Molecular Clouds. ARA&A, 41, 57–115.
- Lane, J., Kirk, H., Johnstone, D., Mairs, S., Di Francesco, J., Sadavoy, S., Hatchell, J., Berry, D. S., Jenness, T., Hogerheijde, M. R., Ward-Thompson, D., and The JCMT Gould Belt Survey Team. 2016. The JCMT Gould Belt Survey: Dense Core Clusters in Orion A. ApJ, 833(Dec.), 44.
- Larson, R. B. 1998. Early star formation and the evolution of the stellar initial mass function in galaxies. MNRAS, 301(Dec.), 569–581.
- Lee, J. C., Gil de Paz, A., Tremonti, C., Kennicutt, Jr., R. C., Salim, S., Bothwell, M., Calzetti, D., Dalcanton, J., Dale, D., Engelbracht, C., Funes, S. J. J. G., Johnson, B., Sakai, S., Skillman, E., van Zee, L., Walter, F., and Weisz, D. 2009. Comparison of $H\alpha$ and UV Star Formation Rates in the Local Volume: Systematic Discrepancies for Dwarf Galaxies. ApJ, **706**(Nov.), 599–613.
- Lelli, F., Verheijen, M., and Fraternali, F. 2014. Dynamics of starbursting dwarf galaxies. III. A H I study of 18 nearby objects. A&A, **566**(June), A71.
- Lelli, F., McGaugh, S. S., Schombert, J. M., and Pawlowski, M. S. 2017. One Law to Rule Them All: The Radial Acceleration Relation of Galaxies. ApJ, 836(Feb.), 152.
- Lieberz, P., and Kroupa, P. 2017. On the origin of the Schechter-like mass function of young star clusters in disc galaxies. MNRAS, 465(Mar.), 3775–3783.
- Lim, B., Sung, H., Bessell, M. S., Lee, S., Lee, J. J., Oh, H., Hwang, N., Park, B.-G., Hur, H., Hong, K., and Park, S. 2018. Kinematic evidence for feedback-driven star formation in NGC 1893. *MNRAS*, 477(June), 1993–2003.
- Lin, Y., Csengeri, T., Wyrowski, F., Urquhart, J. S., Schuller, F., Weiss, A., and Menten, K. M. 2019. Fragmentation and filaments at the onset of star and cluster formation. SABOCA 350 μ m view of ATLASGAL-selected massive clumps. $A \mathcal{E} A$, **631**(Nov.), A72.
- Liptai, D., Price, D. J., Wurster, J., and Bate, M. R. 2017. Does turbulence determine the initial mass function? *MNRAS*, **465**(Feb.), 105–110.
- Mahajan, Smriti, Ashby, M. L. N., Willner, S. P., Barmby, P., Fazio, G. G., Maragkoudakis, A., Raychaudhury, S., and Zezas, A. 2019. The Star Formation Reference Survey III. A multiwavelength view of star formation in nearby galaxies. MNRAS, 482(Jan.), 560–577.

- Maíz Apellániz, J., Walborn, Nolan R., Morrell, N. I., Niemela, V. S., and Nelan, E. P. 2007. Pismis 24-1: The Stellar Upper Mass Limit Preserved. *ApJ*, **660**(2), 1480–1485.
- Marks, M., and Kroupa, P. 2012. Inverse dynamical population synthesis. Constraining the initial conditions of young stellar clusters by studying their binary populations. $A \mathcal{E} A$, $\mathbf{543}(\mathrm{July})$, A8.
- Marks, M., Kroupa, P., and Oh, S. 2011. An analytical description of the evolution of binary orbital-parameter distributions in N-body computations of star clusters. MNRAS, 417(Nov.), 1684–1701.
- Marks, M., Kroupa, P., Dabringhausen, J., and Pawlowski, M. S. 2012. Evidence for top-heavy stellar initial mass functions with increasing density and decreasing metallicity. MNRAS, 422(May), 2246–2254.
- Martín-Navarro, I. 2016. Revisiting the classics: is [Mg/Fe] a good proxy for galaxy formation time-scales? MNRAS, 456(Feb.), L104–L108.
- Maschberger, T., and Clarke, C. J. 2008. Maximum stellar mass versus cluster membership number revisited. *MNRAS*, **391**(Dec.), 711–717.
- Massey, P. 2003. MASSIVE STARS IN THE LOCAL GROUP: Implications for Stellar Evolution and Star Formation. ARA&A, 41, 15–56.
- Matteucci, F. 1994. Abundance ratios in ellipticals and galaxy formation. A & A, **288**(Aug.), 57–64.
- Matzner, C. D., and McKee, C. F. 2000. Efficiencies of Low-Mass Star and Star Cluster Formation. *ApJ*, **545**(Dec.), 364–378.
- McGaugh, S. S. 2004. The Mass Discrepancy-Acceleration Relation: Disk Mass and the Dark Matter Distribution. *ApJ*, **609**(July), 652–666.
- McGaugh, S. S. 2005. The Baryonic Tully-Fisher Relation of Galaxies with Extended Rotation Curves and the Stellar Mass of Rotating Galaxies. *ApJ*, **632**(Oct.), 859–871.
- McGaugh, S. S. 2012. The Baryonic Tully-Fisher Relation of Gas-rich Galaxies as a Test of Λ CDM and MOND. AJ, **143**(Feb.), 40.
- McGaugh, S. S., Lelli, F., and Schombert, J. M. 2016. Radial Acceleration Relation in Rotationally Supported Galaxies. *Physical Review Letters*, **117**(20), 201101.
- McQuinn, K. B. W., Skillman, E. D., Dolphin, A., Cannon, J. M., Salzer, J. J., Rhode, K. L., Adams, E. A. K., Berg, D., Giovanelli, R., Girardi, L., and Haynes, M. P. 2015. Leo P: An Unquenched Very Low-mass Galaxy. *ApJ*, **812**(Oct.), 158.
- McQuinn, K. B. W., Skillman, E. D., Heilman, T. N., Mitchell, N. P., and Kelley, T. 2018. Galactic outflows, star formation histories, and time-scales in starburst dwarf galaxies from STARBIRDS. *MNRAS*, 477(July), 3164–3177.
- Megeath, S. T., Gutermuth, R., Muzerolle, J., Kryukova, E., Flaherty, K., Hora, J. L., Allen, L. E., Hartmann, L., Myers, P. C., Pipher, J. L., Stauffer, J., Young, E. T., and Fazio, G. G. 2012. The Spitzer Space Telescope Survey of the Orion A and B Molecular Clouds. I. A Census of Dusty Young Stellar Objects and a Study of Their Mid-infrared Variability. AJ, 144(Dec.), 192.
- Megeath, S. T., Gutermuth, R., Muzerolle, J., Kryukova, E., Hora, J. L., Allen, L. E., Flaherty, K., Hartmann, L., Myers, P. C., Pipher, J. L., Stauffer, J., Young, E. T., and Fazio, G. G. 2016. The Spitzer Space Telescope Survey of the Orion A and B Molecular Clouds. II. The Spatial Distribution and Demographics of Dusty Young Stellar Objects. *AJ*, **151**(Jan.), 5.
- Meurer, G. R., Wong, O. I., Kim, J. H., Hanish, D. J., Heckman, T. M., Werk, J., Bland-Hawthorn, J., Dopita, M. A., Zwaan, M. A., Koribalski, B., Seibert,

- M., Thilker, D. A., Ferguson, H. C., Webster, R. L., Putman, M. E., Knezek, P. M., Doyle, M. T., Drinkwater, M. J., Hoopes, C. G., Kilborn, V. A., Meyer, M., Ryan-Weber, E. V., Smith, R. C., and Staveley-Smith, L. 2009. Evidence for a Nonuniform Initial Mass Function in the Local Universe. *ApJ*, **695**(Apr.), 765–780.
- Miller, G. E., and Scalo, J. M. 1979. The initial mass function and stellar birthrate in the solar neighborhood. ApJS, 41(Nov.), 513–547.
- Mor, R., Robin, A. C., Figueras, F., and Lemasle, B. 2017. Constraining the thin disc initial mass function using Galactic classical Cepheids. A & A, 599(Mar.), A17.
- Mor, R., Robin, A. C., Figueras, F., and Antoja, T. 2018. BGM FASt: Besançon Galaxy Model for big data. Simultaneous inference of the IMF, SFH, and density in the solar neighbourhood. $A \mathcal{E}A$, **620**(Dec.), A79.
- Oey, M. S., and Clarke, C. J. 2005. Statistical Confirmation of a Stellar Upper Mass Limit. ApJ, **620**(Feb.), L43–L46.
- Offner, S. S. R., Clark, P. C., Hennebelle, P., Bastian, N., Bate, M. R., Hopkins, P. F., Moraux, E., and Whitworth, A. P. 2014. The Origin and Universality of the Stellar Initial Mass Function. *Protostars and Planets VI*, 53–75.
- Oh, S., and Kroupa, P. 2012. The influence of stellar dynamical ejections and collisions on the relation between the maximum stellar and star cluster mass. *MNRAS*, **424**(July), 65–79.
- Oh, S., and Kroupa, P. 2016. Dynamical ejections of massive stars from young star clusters under diverse initial conditions. $A \mathcal{E} A$, 590(May), A107.
- Oh, S., and Kroupa, P. 2018. Very massive stars in not so massive clusters. *MNRAS*, **481**(Nov.), 153–163.
- Oh, S., Kroupa, P., and Pflamm-Altenburg, J. 2015. Dependency of Dynamical Ejections of O Stars on the Masses of Very Young Star Clusters. *ApJ*, **805**(June), 92.
- Padoan, P., and Nordlund, Å. 2002. The Stellar Initial Mass Function from Turbulent Fragmentation. ApJ, 576(Sept.), 870–879.
- Papadopoulos, P. P., and Thi, W.-F. 2013. The Initial Conditions of Star Formation: Cosmic Rays as the Fundamental Regulators. Page 41 of: Torres, D. F., and Reimer, O. (eds), *Cosmic Rays in Star-Forming Environments*. Advances in Solid State Physics, vol. 34.
- Parker, R. J., and Goodwin, S. P. 2007. Do O-stars form in isolation? *MNRAS*, **380**(Sept.), 1271–1275.
- Pavlík, Václav, Kroupa, Pavel, and Šubr, Ladislav. 2019. Do star clusters form in a completely mass-segregated way? $A\mathcal{C}A$, **626**(Jun), A79.
- Pflamm-Altenburg, J., and Kroupa, P. 2006. A highly abnormal massive star mass function in the Orion Nebula cluster and the dynamical decay of trapezium systems. *MNRAS*, **373**(Nov.), 295–304.
- Pflamm-Altenburg, J., and Kroupa, P. 2008. Clustered star formation as a natural explanation for the H α cut-off in disk galaxies. *Nature*, **455**(Oct.), 641–643.
- Pflamm-Altenburg, J., and Kroupa, P. 2009. The Fundamental Gas Depletion and Stellar-Mass Buildup Times of Star-Forming Galaxies. *ApJ*, **706**(Nov.), 516–524.
- Pflamm-Altenburg, J., and Kroupa, P. 2010. The two-step ejection of massive stars and the issue of their formation in isolation. MNRAS, 404(May), 1564–1568.
- Pflamm-Altenburg, J., Weidner, C., and Kroupa, P. 2007. Converting H α Luminosities into Star Formation Rates. ApJ, **671**(Dec.), 1550–1558.

- Pflamm-Altenburg, J., Weidner, C., and Kroupa, P. 2009. Diverging UV and H α fluxes of star-forming galaxies predicted by the IGIMF theory. MNRAS, **395**(May), 394–400.
- Pflamm-Altenburg, J., González-Lópezlira, R. A., and Kroupa, P. 2013. The galactocentric radius dependent upper mass limit of young star clusters: stochastic star formation ruled out. *MNRAS*, **435**(Nov.), 2604–2609.
- Plummer, H. C. 1911. On the problem of distribution in globular star clusters. MNRAS, **71**(Mar.), 460–470.
- Plunkett, A. L., Fernández-López, M., Arce, H. G., Busquet, G., Mardones, D., and Dunham, M. M. 2018. Distribution of Serpens South protostars revealed with ALMA. $A \mathcal{E} A$, **615**(July), A9.
- Portail, M., Wegg, C., Gerhard, O., and Ness, M. 2017. Chemodynamical modelling of the galactic bulge and bar. MNRAS, 470(Sept.), 1233–1252.
- Ramírez Alegría, S., Borissova, J., Chené, A.-N., Bonatto, C., Kurtev, R., Amigo, P., Kuhn, M., Gromadzki, M., and Carballo-Bello, J. A. 2016. Massive open star clusters using the VVV survey. V. Young clusters with an OB stellar population. A & A, 588(Apr.), A40.
- Randriamanakoto, Z., Escala, A., Väisänen, P., Kankare, E., Kotilainen, J., Mattila, S., and Ryder, S. 2013. Near-infrared Adaptive Optics Imaging of Infrared Luminous Galaxies: The Brightest Cluster Magnitude-Star Formation Rate Relation. *ApJ*, **775**(Oct.), L38.
- Randriamanakoto, Z., Väisänen, P., Ryder, S. D., and Ranaivomanana, P. 2018. Young massive clusters in the interacting LIRG Arp 299: evidence for the dependence of star cluster formation and evolution on environment. *MNRAS*, Oct.
- Recchi, S., and Kroupa, P. 2015. The chemical evolution of galaxies with a variable integrated galactic initial mass function. *MNRAS*, **446**(Feb.), 4168–4175.
- Recchi, S., Calura, F., and Kroupa, P. 2009. The chemical evolution of galaxies within the IGIMF theory: the [α /Fe] ratios and downsizing. $A \mathcal{E} A$, 499(June), 711–722.
- Riedel, A. R., Silverstein, M. L., Henry, T. J., Jao, W.-C., Winters, J. G., Subasavage, J. P., Malo, L., and Hambly, N. C. 2018. The Solar Neighborhood. XLIII. Discovery of New Nearby Stars with mu¡0.18/yr (TINYMO Sample). *AJ*, **156**(Aug.), 49.
- Rybizki, J., and Just, A. 2015. Towards a fully consistent Milky Way disc model III. Constraining the initial mass function. MNRAS, 447(Mar.), 3880–3891.
- Salpeter, E. E. 1955. The Luminosity Function and Stellar Evolution. ApJ, ${\bf 121}({\rm Jan.}), 161.$
- Sana, H., de Mink, S. E., de Koter, A., Langer, N., Evans, C. J., Gieles, M., Gosset, E., Izzard, R. G., Le Bouquin, J.-B., and Schneider, F. R. N. 2012. Binary Interaction Dominates the Evolution of Massive Stars. Science, 337(July), 444.
- Scalo, J. M. 1986. The stellar initial mass function. Fundamentals of Cosmic Physics, 11(May), 1–278.
- Schneider, F. R. N., Izzard, R. G., de Mink, S. E., Langer, N., Stolte, A., de Koter, A., Gvaramadze, V. V., Hußmann, B., Liermann, A., and Sana, H. 2014. Ages of Young Star Clusters, Massive Blue Stragglers, and the Upper Mass Limit of Stars: Analyzing Age-dependent Stellar Mass Functions. *ApJ*, **780**(Jan.), 117.

- Schneider, F. R. N., Izzard, R. G., Langer, N., and de Mink, S. E. 2015. Evolution of Mass Functions of Coeval Stars through Wind Mass Loss and Binary Interactions. ApJ, 805(May), 20.
- Schneider, F. R. N., Sana, H., Evans, C. J., Bestenlehner, J. M., Castro, N., Fossati, L., Gräfener, G., Langer, N., Ramírez-Agudelo, O. H., Sabín-Sanjulián, C., Simón-Díaz, S., Tramper, F., Crowther, P. A., de Koter, A., de Mink, S. E., Dufton, P. L., Garcia, M., Gieles, M., Hénault-Brunet, V., Herrero, A., Izzard, R. G., Kalari, V., Lennon, D. J., Maíz Apellániz, J., Markova, N., Najarro, F., Podsiadlowski, P., Puls, J., Taylor, W. D., van Loon, J. T., Vink, J. S., and Norman, C. 2018. An excess of massive stars in the local 30 Doradus starburst. Science, 359(Jan.), 69–71.
- Schneider, N., Csengeri, T., Hennemann, M., Motte, F., Didelon, P., Federrath, C., Bontemps, S., Di Francesco, J., Arzoumanian, D., Minier, V., André, P., Hill, T., Zavagno, A., Nguyen-Luong, Q., Attard, M., Bernard, J.-P., Elia, D., Fallscheer, C., Griffin, M., Kirk, J., Klessen, R., Könyves, V., Martin, P., Men'shchikov, A., Palmeirim, P., Peretto, N., Pestalozzi, M., Russeil, D., Sadavoy, S., Sousbie, T., Testi, L., Tremblin, P., Ward-Thompson, D., and White, G. 2012. Cluster-formation in the Rosette molecular cloud at the junctions of filaments. A&A, 540(Apr.), L11.
- Schulz, C., Pflamm-Altenburg, J., and Kroupa, P. 2015. Mass distributions of star clusters for different star formation histories in a galaxy cluster environment. $A \mathcal{B} A$, **582**(Oct.), A93.
- Shimajiri, Y., André, P., Braine, J., Könyves, V., Schneider, N., Bontemps, S., Ladjelate, B., Roy, A., Gao, Y., and Chen, H. 2017. Testing the universality of the star-formation efficiency in dense molecular gas. $A\mathcal{B}A$, **604**(Aug.), A74.
- Smith, N., Stassun, K. G., and Bally, J. 2005. Opening the Treasure Chest: A Newborn Star Cluster Emerges from Its Dust Pillar in Carina. AJ, 129(Feb.), 888–899.
- Smith, R. J. 2014. Variations in the initial mass function in early-type galaxies: a critical comparison between dynamical and spectroscopic results. MNRAS, 443(Sept.), L69–L73.
- Smith, R. J., and Lucey, J. R. 2013. A giant elliptical galaxy with a lightweight initial mass function. *MNRAS*, **434**(Sept.), 1964–1977.
- Speagle, J. S., Steinhardt, C. L., Capak, P. L., and Silverman, J. D. 2014. A Highly Consistent Framework for the Evolution of the Star-Forming "Main Sequence" from z ~ 0-6. ApJS, 214(Oct.), 15.
- Stephens, I. W., Gouliermis, D., Looney, L. W., Gruendl, R. A., Chu, Y.-H., Weisz, D. R., Seale, J. P., Chen, C.-H. R., Wong, T., Hughes, A., Pineda, J. L., Ott, J., and Muller, E. 2017. Stellar Clusterings around "Isolated" Massive YSOs in the LMC. ApJ, 834(Jan.), 94.
- Thies, I., Pflamm-Altenburg, J., Kroupa, P., and Marks, M. 2015. Characterizing the Brown Dwarf Formation Channels from the Initial Mass Function and Binary-star Dynamics. ApJ, 800(Feb.), 72.
- Thomas, D., Maraston, C., Bender, R., and Mendes de Oliveira, C. 2005. The Epochs of Early-Type Galaxy Formation as a Function of Environment. *ApJ*, **621**(Mar.), 673–694.
- Tsujimoto, T. 2011. Chemical Signature Indicating a Lack of Massive Stars in Dwarf Galaxies. ApJ, **736**(Aug.), 113.
- Urquhart, J. S., Figura, C. C., Moore, T. J. T., Hoare, M. G., Lumsden, S. L., Mottram, J. C., Thompson, M. A., and Oudmaijer, R. D. 2014. The RMS

- survey: galactic distribution of massive star formation. MNRAS, 437(Jan.), 1791–1807.
- Šubr, L., Kroupa, P., and Baumgardt, H. 2008. A new method to create initially mass segregated star clusters in virial equilibrium. *MNRAS*, **385**(Apr.), 1673–1680.
- van Dokkum, P. G., and Conroy, C. 2010. A substantial population of low-mass stars in luminous elliptical galaxies. *Nature*, **468**(Dec.), 940–942.
- Vanbeveren, D. 1982. On the difference between the initial mass function of single stars and of primaries of binaries. $A \mathcal{E}A$, 115(Nov.), 65–68.
- Vazdekis, A., Peletier, R. F., Beckman, J. E., and Casuso, E. 1997. A New Chemoevolutionary Population Synthesis Model for Early-Type Galaxies. II. Observations and Results. *ApJS*, **111**(July), 203–232.
- Wang, Long, Kroupa, Pavel, and Jerabkova, Tereza. 2019. Complete ejection of OB stars from very young star clusters and the formation of multiple populations. *MNRAS*, **484**(2), 1843–1851.
- Watts, A. B., Meurer, G. R., Lagos, C. D. P., Bruzzese, S. M., Kroupa, P., and Jerabkova, T. 2018. Star formation in the outskirts of DDO 154: a top-light IMF in a nearly dormant disc. *MNRAS*, 477(July), 5554–5567.
- Wegg, C., Gerhard, O., and Portail, M. 2017. The Initial Mass Function of the Inner Galaxy Measured from OGLE-III Microlensing Timescales. *ApJ*, **843**(July), L5.
- Weidner, C., and Kroupa, P. 2004. Evidence for a fundamental stellar upper mass limit from clustered star formation. MNRAS, 348(Feb.), 187–191.
- Weidner, C., and Kroupa, P. 2005. The Variation of Integrated Star Initial Mass Functions among Galaxies. *ApJ*, **625**(June), 754–762.
- Weidner, C., and Kroupa, P. 2006. The maximum stellar mass, star-cluster formation and composite stellar populations. *MNRAS*, **365**(Feb.), 1333–1347.
- Weidner, C., Kroupa, P., and Larsen, S. S. 2004. Implications for the formation of star clusters from extragalactic star formation rates. *MNRAS*, **350**(June), 1503–1510.
- Weidner, C., Kroupa, P., and Maschberger, T. 2009. The influence of multiple stars on the high-mass stellar initial mass function and age dating of young massive star clusters. *MNRAS*, **393**(Feb.), 663–680.
- Weidner, C., Kroupa, P., and Bonnell, I. A. D. 2010. The relation between the most-massive star and its parental star cluster mass. *MNRAS*, **401**(Jan.), 275–293.
- Weidner, C., Ferreras, I., Vazdekis, A., and La Barbera, F. 2013a. The (galaxy-wide) IMF in giant elliptical galaxies: from top to bottom. *MNRAS*, **435**(Nov.), 2274–2280.
- Weidner, C., Kroupa, P., Pflamm-Altenburg, J., and Vazdekis, A. 2013b. The galaxy-wide initial mass function of dwarf late-type to massive early-type galaxies. *MNRAS*, **436**(Dec.), 3309–3320.
- Weidner, C., Kroupa, P., and Pflamm-Altenburg, J. 2013c. The m_{max} - M_{ecl} relation, the IMF and IGIMF: probabilistically sampled functions. MNRAS, 434(Sept.), 84–101.
- Weidner, Carsten, Kroupa, Pavel, and Pflamm-Altenburg, Jan. 2014. Sampling methods for stellar masses and the m_{max} - M_{ecl} relation in the starburst dwarf galaxy NGC 4214. MNRAS, 441(4), 3348–3358.

- Whitmore, B. C., Zhang, Q., Leitherer, C., Fall, S. M., Schweizer, F., and Miller, B. W. 1999. The Luminosity Function of Young Star Clusters in "the Antennae" Galaxies (NGC 4038-4039). AJ, 118(Oct.), 1551–1576.
- Wright, N. J., and Mamajek, E. E. 2018. The kinematics of the Scorpius-Centaurus OB association from Gaia DR1. MNRAS, 476(May), 381–398.
- Wuchterl, G., and Tscharnuter, W. M. 2003. From clouds to stars. Protostellar collapse and the evolution to the pre-main sequence I. Equations and evolution in the Hertzsprung-Russell diagram. A&A, 398(Feb.), 1081–1090.
- Yan, Z., Jerabkova, T., and Kroupa, P. 2017. The optimally sampled galaxy-wide stellar initial mass function. Observational tests and the publicly available GalIMF code. $A \mathcal{E}A$, 607(Nov.), A126.
- Yan, Zhiqiang, Jeřábková, Tereza, and Kroupa, Pavel. 2021. Downsizing revised: Star formation timescales for elliptical galaxies with an environment-dependent IMF and a number of SNIa. $A \mathcal{C}A$, 655(Nov.), A19.
- Zhang, Q., Fall, S. M., and Whitmore, B. C. 2001. A Multiwavelength Study of the Young Star Clusters and Interstellar Medium in the Antennae Galaxies. ApJ, **561**(Nov.), 727–750.
- Zhang, Z.-Y., Romano, D., Ivison, R. J., Papadopoulos, P. P., and Matteucci, F. 2018. Stellar populations dominated by massive stars in dusty starburst galaxies across cosmic time. *Nature*, **558**(June), 260–263.
- Zinnecker, H., and Yorke, H. W. 2007. Toward Understanding Massive Star Formation. ARA&A, 45(Sept.), 481–563.
- Zonoozi, A. H., Haghi, H., and Kroupa, P. 2016. A Possible Solution for the M/L-[Fe/H] Relation of Globular Clusters in M3. I. A Metallicity- and Densitydependent Top-heavy IMF. ApJ, 826(July), 89.
- Zonoozi, Akram Hasani, Mahani, Hamidreza, and Kroupa, Pavel. 2019. Was the Milky Way a chain galaxy? Using the IGIMF theory to constrain the thin-disc star formation history and mass. *MNRAS*, **483**(1), 46–56.